Characterization of Pressure-Induced Anisotropy in Atactic Polystyrene

By

Derek Rott

ScB., Brown University 2018

Thesis

Submitted in partial fulfilment of the requirements of the Degree of Masters of Science in the Department of Molecular Pharmacology, Physiology, and Biotechnology at Brown University

PROVIDENCE, RHODE ISLAND

MAY 2019

AUTHORIZATION TO LEND AND REPRODUCE THIS THESIS

As the sole author of this thesis, I authorize Brown University to lend it to other institutions or individuals for the purpose of scholarly research.

Date:_____ Signature: _____

Derek Rott, Author

I further authorize Brown University to reproduce this thesis by photocopying or other means, in total or in part, at the request of other institutions or individuals for the purpose of scholarly research.

Date:_____ Signature: _____

Derek Rott, Author

This thesis by Derek M. Rott is accepted in its present form by the Department of Molecular Pharmacology Physiology and Biotechnology as satisfying the thesis requirement for the degree of Master of Science.

Date_____ _____

Dr. Edith Mathiowitz, Advisor

Recommended to the Graduate Council

Date_____ _____

Dr. Edith Mathiowitz, Reader

Date_____ _____

Dr. Anita Shukla, Reader

Date_____ _____

Dr. Diana Horrigan, Reader

Approved by the Graduate Council

Date_____ _____

Dr. Andrew Campbell, Dean of the Graduate School

Acknowledgements

I extend my sincere gratitude to my advisor, Dr. Edith Mathiowitz, for making my work possible and helping me develop as a scientist. I thank Cameron Baptista for the technical training and the continued insight he provided over the course of this research. I thank Hector Garces for his assistance with training and operating the X-ray diffraction instrument. I also extend my thanks to the members of the Mathiowitz laboratory group, especially Sheila Velagapudi, Aharon Azagury, and Stacia Furtado, for contributing their time and advice to my project.

Finally, I would like to offer my gratitude to the family and friends who have supported me throughout my degree. You all made this possible.

Table of Contents

List of Tables

List of Figures

Introduction

Morphology and Physical Properties of Polymers

Polymers can be broadly classified based on their morphologies as semi-crystalline or amorphous. Amorphous polymers consist of disordered inter-tangled chains. Semi-crystalline polymers contain highly ordered lamellae – aligned portions of multiple polymer chains interconnected by amorphous regions.[1] The formation of crystalline regions is primarily controlled by the reduction in chain conformational entropy and whether the enthalpy of secondary bond formation exceeds the free energy barriers to crystallization.[2] Therefore, the characteristics of the side groups are key to determining the extent of crystallinity in a polymer. Large side groups may disrupt ordered packing of the chain, decreasing the likelihood of crystallization while secondary interactions such as hydrogen bonding and Van der Waals interactions can increase the degree of crystallinity. Stereoregularity – how the side groups are oriented relative to the backbone – plays an important role as well. Isotactic and syndiotactic polymers, such as in the forms of polystyrene shown in **Figure 1**, tend to exhibit more crystallinity than atactic polymers which have randomly distributed side chains. While no polymer can be entirely crystalline, the relative degree of crystallinity in bulk polymer can have effects on supermolecular structure and physical properties.

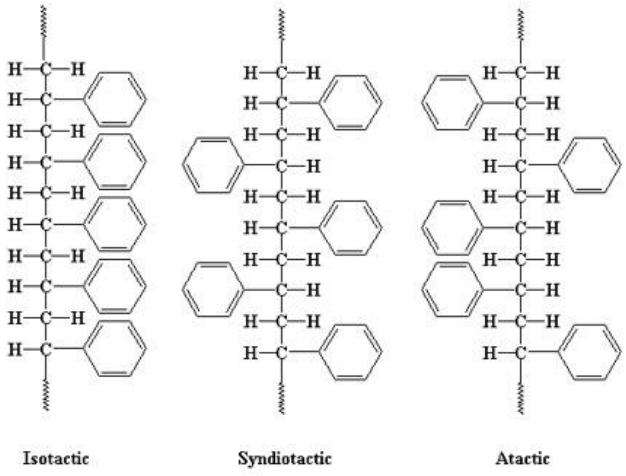

Fig. 1. Schematic view of isotactic, syndiotactic, and atactic polystyrene.[1]

The differences in physical properties between amorphous and semi-crystalline polymers are primarily due to lamellae. These tightly packed regions of polymer chain result in greater density, mechanical strength, and brittleness of the bulk material by increasing the number and density of secondary polymer interactions. The melt temperature (T_m) is the temperature at which the entropic gains of having free polymer chains outweigh the energy released by secondary bond formation within the lamellae, resulting in crystal melt. The amorphous regions of semi-crystalline and amorphous polymers exhibit a glass transition temperature (T_g) where below this temperature, the polymer behaves like a glass and above which it behaves rubbery. This is because below T_g, molecular motion is limited to vibrations of atoms about equilibrium positions with little main chain and side group motion; temperatures above T_g allow cooperative movement of polymer segments and flow.[1]

In addition to highly oriented crystal phases and disordered amorphous phases, regions of polymer can adopt an intermediate mesophase morphology. A polymer mesophase occurs when amorphous regions become partially oriented along a single axis and develop anisotropic – directionally-dependent – properties. In contrast to the high degree of positional and orientational order found in crystalline regions, mesophases lack the characteristic lamellae. However, mesophase polymers frequently exhibit increased mechanical strength along the axis of alignment compared to amorphous polymers.[1,3] This semi-ordered nature also can result in birefringence, a form of optical anisotropy where a plane of polarized light is rotated a discrete angle by ordered structures and is distinct from the isotropic scattering of lamellae. Mesophases can be the result of different physical processing techniques or inherent to the polymer structure.

Processing-Induced Anisotropy

Mesophases can be induced through mechanical stretching and techniques that align flowing polymer chains. This mechanical processing involves applying tensile stress to a polymer along one or two axes; amorphous regions will align first because of their weaker secondary bonds, then the lamellae become aligned along the axis.[4] This induces optical and mechanical anisotropy. These anisotropic affects are present in samples stretched above and below the T_g of the polymer, but the anisotropy relaxes and dissipates in polymers stretched below the T_g and in those stretched above the T_g where the stress is removed while at the elevated temperature.[5-8] The anisotropic properties can be preserved for longer time periods using a "frozen stress" procedure where the cooling occurs while the stress is maintained.[7] Flow techniques, which include extrusion molding and fiber spinning, use polymer that has either been heated such that it can flow or dissolved in solvent. In this more labile state, the material is either forced through a die or drawn through a spinneret. This partially aligns the polymer strands through shear flow prior to cooling or solvent evaporation, locking in the morphology.[1] These processes achieve anisotropic optical and mechanical properties as in stretching, but are only used for linearly extruded products like fibers, films, and thermoplastics with uniform cross-sections such as tubing.

Another potential method for inducing mesophases in non-mesogenic polymers is compression at elevated temperatures, referred to here as hot-pressing. This process involves heating the polymer to a desired temperature, applying a given pressure for a set time at the elevated pressure, and then cooling the polymer while maintaining the pressure before ejecting the material. Previous experiments examining hot-pressed poly-L-lactic acid (PLA) morphology using a range of quantitative techniques found that the PLA samples had multiple endotherms

through the T_g range indicating multiple induced morphologies as well as birefringence along multiple angles suggesting optical anisotropy along at least two axes.[9] However, no changes in crystallinity were observed. This led to the conclusion that hot-pressing may induce mesophases in PLA.[9] Additional characterization and quantification of the thermal transitions of the PLA mesophase supporting the hypothesis that the mesophase enhanced crystal formation and were similar to mesophases formed by uniaxial flow processing of PLA.[10] In contrast, hot-pressing experiments studying syndiotactic polystyrene (sPS) found changes in total crystallinity and crystal composition.[11] The differences in observations across different polymers point to a gap in scientific understanding of how hot-pressing effects polymer behavior.

Mesophases as Precursors to Crystallinity

There is scientific interest in how high pressures effect thermal transitions in polymers and the role mesophases play in crystallinity kinetics. In general, increased pressure at elevated temperatures is associated with increases in T_m – at least while the pressure is continually applied. Experiments examining poly-4-methyl pentene-1, *n*-alkanes, high and low density polyethylene, nylon 6, poly(butylene terephthalate), and isotactic polypropylene using high-pressure differential scanning calorimetry and high-pressure Differential Thermal Analysis have reported this relationship.[12-14] However, this behavior is not present in all crystal phases, such as the decrease in T_m of the less dense α crystal phase and the increase in T_m of the more dense β crystal phase observed in hot-pressed sPS.[11] The role of pressure and the hot-pressing process on the T_g of polymers is even less defined, though it has been reported that pressurized atactic polystyrene (aPS) shows an increase in T_g approaching a theoretical maximum under high pressures, and hot-pressed sPS has been reported to have elevated T_g correlating with increased

pressure.[11,15] Many of these studies seek to elucidate properties of crystallization kinetics as opposed to producing materials with advantageous mechanical properties.

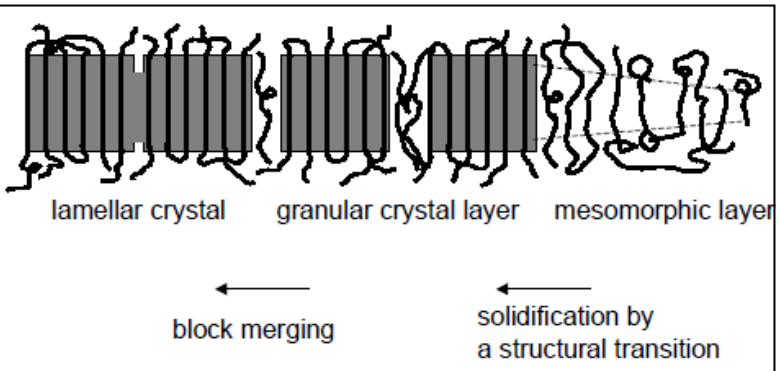

Fig. 2. The proposed route for polymer crystal formation by addition of mesophase blocks.[16]

It is hypothesized that mesophases play a crucial role in crystallization from the melt, though the extent of this effect is still debated. The model proposed by Strobl, referenced in **Figure 2**, posits that a mesomorphic state is formed prior to crystallization and that blocks of this state are attached to the crystal growth front to form lamellae.[16] This theory has been supported by atomic force microscopy (AFM) showing the granular makeup of polymer lamellae, the observation of a hexatic phase in n-alkanes, and theoretical modeling.[16,17] The role of shear flow-induced mesophases at elevated temperatures on crystallization has also been investigated. Studies employing small-angle and wide-angle X-ray spectroscopy show the formation of oriented precursors to "shish kebab" crystallized structures in isotactic polypropylene (iPP), even at temperatures above the nominal T_m.[18,19] Similar shear flow-induced anisotropic structures were also observed via polarized optical microscopy and depolarized light scattering (DPLS) in isotactic polystyrene (iPS) between 210 and 250C, resulting in crystallization at temperatures below its T_m (223°C).[20] The information on mesophases' role in polymer crystallization is far from conclusive, but this line of research shows promise.

Motivation for Studying Atactic Polystyrene

Atactic polystyrene has potential as a model polymer for studying the effects of hot-pressing on mesophase formation and the role of mesophases in crystal formation. While the effects of hot-pressing aPS are largely unexplored, the stretch-induced photoelastic properties of this entirely amorphous polymer has been researched extensively.[3,5-8,21,22]

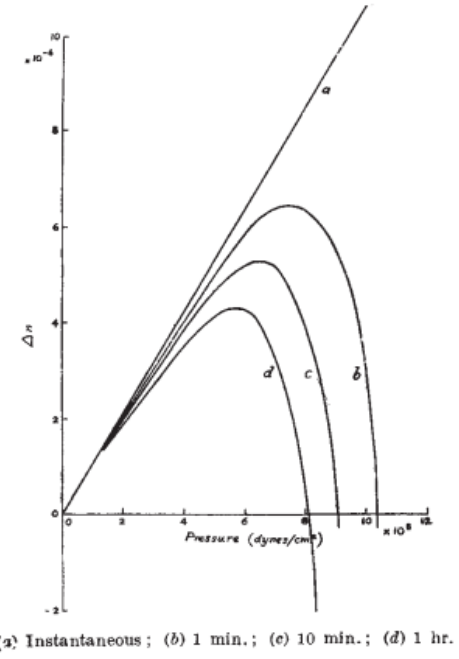

(a) Instantaneous; (b) 1 min.; (c) 10 min.; (d) 1 hr.

Fig. 3. The 'stress-optical' coefficient at 16°C as a function of pressure (dynes/cm^2) over different time periods: (a) Instantaneous. (b) 1 min. (c) 10 min. (d) 1hr.[21]

aPS develops both optical and mechanical anisotropic properties when subjected to mechanical drawing. Mechanical stretch experiments show aPS's 'stress-optical coefficient' – a measure of the relative amounts of positive and negative birefringence shown in **Figure 3** – is dependent on temperature, pressure, and time.[5,6,8,21] Positive birefringence refers to when a plane of polarized light is rotated in the positive direction, corresponding to the alignment of the polymer backbone, as shown in **Figure 4.b**. This form predominates at room temperature and instantaneous stress applications. Negative birefringence – which occurs at elevated temperatures, longer stress application time, and higher pressures – refers to the orientation of the phenyl side perpendicular to the direction of the polymer chains, as shown in **Figure 4.c.**[6] The alignment of the side groups produces a larger optical effect that results in a net rotation of polarized light in the negative direction. Both forms of optical anisotropy were shown to decrease over time, corresponding to a return to an entirely amorphous state once the stress is released unless a "frozen stress" technique

is applied.[5,6,21] The robust photoelastic characterization permits insight into the physical structures formed by aPS hot-pressing and whether it produces a similar effect to "frozen stress" mechanical drawing.

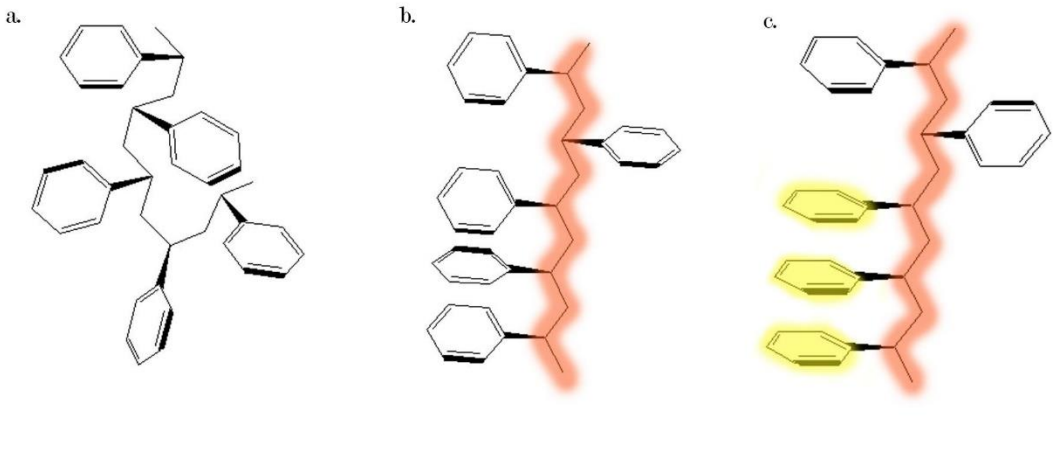

Fig. 4. (a) aPS under insufficient stress to cause alignment **(b)** positive birefringence (red) induced by alignment of carbon backbone by mechanical stretching **(c)** negative birefringence (yellow) induced by "stacking" of styrene side chains perpendicular to aPS backbone under larger stresses, elevated temperatures, and longer stress times

The study of meta-stable anisotropic aPS structures could further elucidate the nature of iPS crystallization as well. In experiments measuring iPS exposed to pulse shear flow at different temperatures described earlier, the optically anisotropic streak structures believed to be precursors to the "shish kebab" crystal form condensed into spherulites exhibiting isotropic scattering after approximately 500s.[20] Because aPS cannot condense into a crystal form, any stable mesophase it might form could serve as an experimental analogue for studying iPS.

Finally, aPS has many commercial applications in the automotive, appliance, electronics, medical, and packaging fields because it is nontoxic, inert, and inexpensive to synthesize. Biaxial mechanical drawing of aPS at 120°C has been reported to double the tensile strength along the axes of stretching.[3] If hot-pressing induces similar meta-stable alignment, further stress-strain

tests can be performed comparing the tensile strength of hot-pressed aPS against other processed forms. Having access to aPS with a radially dispersed anisotropic increase in mechanical strength reliably introduced at low cost would likely expand the material's uses.

Background

Differential Scanning Calorimetry

Differential Scanning Calorimetry (DSC) is a commonly used method to elucidate thermal transitions in polymers. It operates by heating or cooling two aluminum pans, one containing a 3 to 10 milligrams of sample and the other containing a reference material, at a set rate and measuring the heat flow to each pan.[1] At T_g, the temperature where polymers transition from glassy to rubbery states, the heat capacity of the sample increases meaning that more heat flow to the sample pan is required to maintain the same temperature as the reference. This change in heat flow is registered as an endothermic step visible on the DSC readout. In semi-crystalline polymers, T_m can also be determined using DSC since more heat is needed to break secondary bonds in crystals. This creates an endothermic peak that returns to the baseline once the melt has concluded. Crystallization can also be observed as an exothermic peak since enthalpy is released as secondary bonds are formed.

Temperature Modulated Differential Scanning Calorimetry (TMDSC) offers additional insights in polymer transitions by differentiating the heat capacity and kinetic components of total heat flow. It operates similarly to DSC, but after reaching a given temperature interval, the temperature is held constant for a time before resuming heating to the next temperature. This process continues in a stepwise pattern throughout the heating process, producing a heat flow curve that can be split into the reversing and non-reversing curves. The reversing curve, which is associated with the heating step, provides information about the specific heat of the material and transitions such as T_g and irreversible melting occurring at T_m.[23] The non-reversing curve contains the data where the temperature is held constant and is associated with slower kinetic

processes such as cold crystallization.[24] The reversing curve is calculated by dividing the first harmonic of the heat flow by the mass and the amplitude of the applied heating rate; the non-reversing curve is the difference between the average heat flow and the reversing heat flow.[13] Calculating both improves sensitivity for detecting weak transitions and can assist in disentangling overlapping transitions, with the disadvantage being that it takes longer to scan.

In this research, TMDSC is used to investigate the effects of hot-pressing on aPS thermal transitions. In general, T_g temperatures are observed to increase at high pressures because of a decrease in the free volume (v_f) of the polymer. v_f is equal to the specific volume (v) minus the volume of the solidly packed molecules (v_s). A larger v_f means that the polymer chains have more space to move resulting in a lower T_g.[1] High pressures reduce v without changing v_s, resulting in an overall decrease in v_f. The increase in T_g of aPS under high pressures has been previously observed using Rayleigh-Brillouin scattering, see **Figure 5**.[15] This research demonstrated that there is a limiting critical value for aPS T_g at high pressures where above that temperature, the flowing polymer cannot be compressed into a glass.[15] The following research attempts to determine whether the elevated T_g can be maintained in aPS if high pressure is applied during the cooling process. However, an increase in aPS T_g may not directly correlate with the presence of a mesophase structure. Processing techniques that induce uniaxial orientation decrease the entropy of the amorphous region; T_g is primarily controlled by chain length, stiffness, internal mobility,

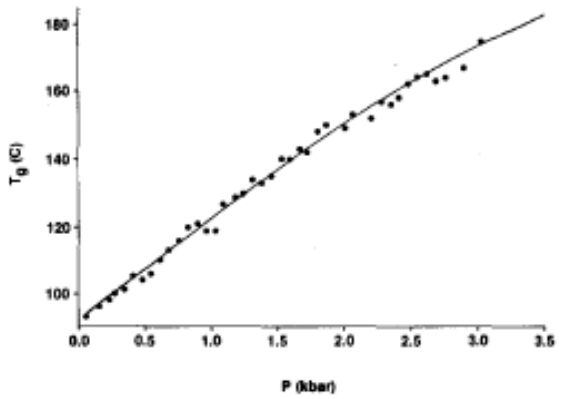

Fig. 5. Values of T_g (°C) vs the pressure P(kbar) as determined by Rayleigh-Brillouin scattering while pressure maintained.[15]

v_f, and attractive forces between polymers.[1] Therefore, mesophase formation coinciding with an increase in T_g would likely only occur if the alignment of amorphous strands increased chain stiffness, limited polymer mobility, or increased inter-chain interactions.

X-Ray Diffraction

X-ray diffraction (XRD) is a procedure that leverages the elastic scattering monochromatic X-rays by electrons to determine the degree of crystallinity, crystal orientation, and crystal structure of the sample.[25] The constructive interference patterns arising from this method are best known to follow Bragg's Law, further explained in **Figure 6**. When analyzing XRD data, changing the Bragg's angle θ changes the set of measured planes, which can provide information on lattice constants that can be used to examine composition and crystal shape.[25] XRD peak intensity is a function of the number of crystallites reflecting X-rays and can be used to calculate the degree of crystallinity. Peak shape accounts for multiple factors but is generally associated with the degree of disorder in a material such that disorder broadens the peak and reduces peak height.[25]

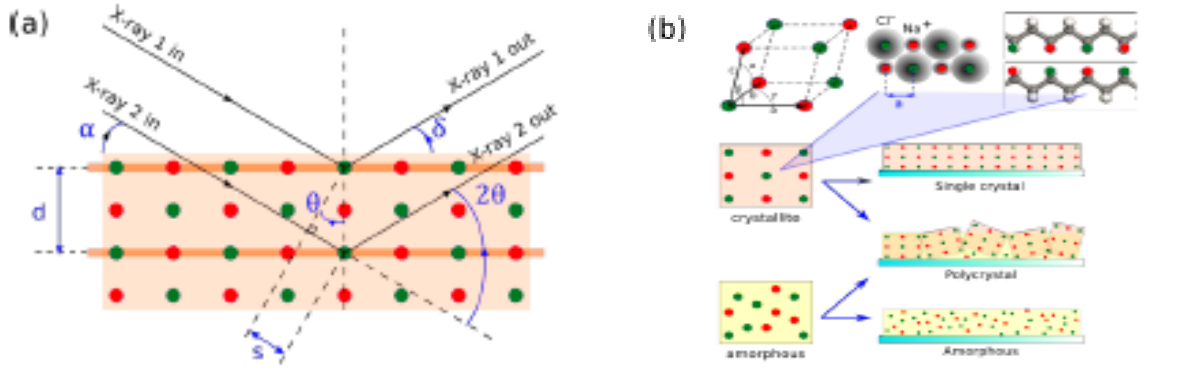

Fig. 6. (a) Constructive interference following *Bragg's Law*: $2d\ sin\theta = m\lambda$ where d is the distance between Bragg's planes, θ is the Bragg's angle, m is the diffraction order, and λ is the wavelength.[25] **(b)** XRD can be used to determine the degree of crystallinity in a sample.

In addition to standard XRD measurements, hot stage XRD is also employed to determine the temperature dependence of ordered and disordered structures. The procedure is identical except for the addition of a heating element on the stage that brings the sample to an equilibrium temperature before each XRD scan. In almost all materials, increased temperature causes more thermal disorder and a decrease in electron density. This is due to thermal expansion which contributes to a broadening and decrease in intensity of XRD peaks.[22] Hot stage XRD can be used on materials with multiple types of crystal regions to determine which structures melt at what temperatures; it can also be used to observe the temperature-dependent behavior of non-crystalline structures.

There are challenges associated with using XRD to study thin films. The first challenge is low signal intensity due to carbon's low atomic number and the thin nature of the samples.[25] This was addressed by increasing the scanning time in order to obtain stronger signals at each θ. The second challenge was that the XRD instrument used in this research was unable to take measurements below 10° without damaging the detector. This prevented the use of small angle or Grazing Incidence XRD methods which tend to reveal additional information in thin films.[25] Therefore, activity occurring at low angles was inferred from the shape of the broad peak associated with aPS styrene side groups.

The XRD spectra of aPS is well characterized and exhibits many unusual features. The entirely amorphous polymer has a spectrum similar to that of styrene with the addition of a smaller "inter-chain" peak at 0.75 $Å^{-1}$ representing the polymer backbone, as shown in **Figure 7.a**.[22] The disproportionate size of the side chain peak, referred to as the "styrene peak," is attributed to the greater cumulative mass and electron density of the styrene side groups. Many portions of the polymer organize into a superchain configuration, shown in **Figure 7.b**, where

the side groups loosely aggregate into disordered non-parallel stacks about the backbone.[22] When the superchain is extended and under favorable energetic conditions, the phenyl groups can self-assort into more oriented stacks similar to the phenyl stacks in semi-crystalline iPS.[22] In aPS, these stacks can contain as many as 6 phenyl groups, but the random monomer distribution in aPS results in 2-4 monomer phenyl stacks predominating.[22] There is a significant energy barrier to forming the stacked structures, accounting for the slow rate of iPS crystallization and the comparatively small amount of highly oriented stacking in aPS. An unusual feature of aPS is that when heated below a threshold temperature, the inter-chain peak observed by XRD increases in intensity because the comparably small and electron-poor region grows proportionally larger than the side chains during thermal expansion.[22] This behavior is irregular given most materials will experience a broadening and shortening of their XRD spectra as the increase in thermal energy decreases structural order.

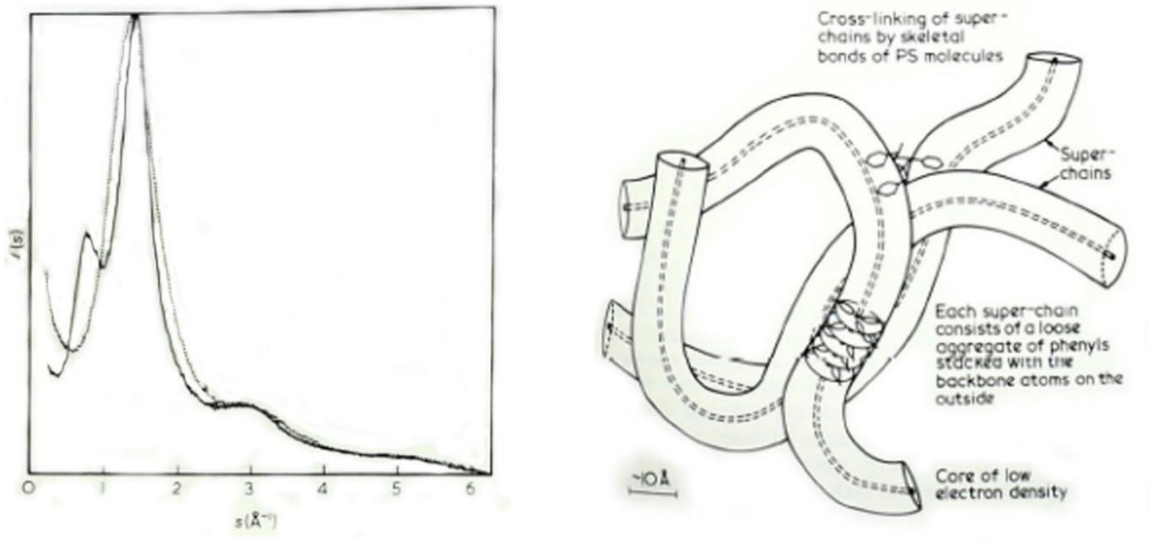

Fig. 7. (a) XRD spectra of aPS (solid line) and liquid styrene (dotted line). The peak at 0.75Å^{-1} is associated with the polymer backbone while the peaks > 1.5Å^{-1} are dependent on the side chain.[22] **(b)** Schematic of the superchain model for aPS: a low electron-density core surrounded by random radially extended phenyl side groups with high electron density. When the superchain is aligned (not tangled), the side groups can form stabilized stacks of up to 6 randomly distributed phenyl groups.[22] Superchains can be linked by aPS chains with side groups intercalating multiple superchains.

Materials and Methods

Sample Preparation

aPS beads, MW 125,000 – 250,000 (CAT 00574), were purchased from Polysciences, Inc. 0.5000 +/- 0.0005 grams of the aPS beads were measured onto weighing paper using a Mettler Toledo X5204 DeltaRange scale; a Workstation Ionizer (Engineered Static Solutions, Inc.) was used while measuring and transferring aPS beads. The material was transferred to a 1" diameter well in a pourable silicone rubber mold (Mold Star 30) containing 5 wells before being placed in a preheated to 180°C StableTemp Oven (Cole Parmer). The oven temperature was kept between 200 - 220°C (below degradation temperatures for aPS and the mold), monitored by an internal thermometer (Lab-Line Instruments, Inc., Melrose Park, IL), and baked for between 1.75 – 2.5 hours. Baking times varied from batch to batch because the samples initially contained gas bubbles that were only removed by increasing baking time. As soon as all samples were bubble-free, the silicone rubber mold was removed from the oven and allowed to slowly cool to room temperature over 45 – 60 minutes on the lab bench. Once at room temperature, the samples were extricated from the mold and imperfections from the casting, such as spurs and runners, were removed using a razor blade.

Hot-Pressing of aPS Samples

Cleaned aPS disks were centered between two 0.048" thick polished mirror-like 304 stainless steel sheets purchased from McMaster-Carr. The hot-pressing procedure, summarized in **Figure 8**, used a Carver Auto Series Hydraulic Press (Carver, Wabash, Indiana) which contains heating and cooling elements on both clamps. The hydraulic press was preheated to the

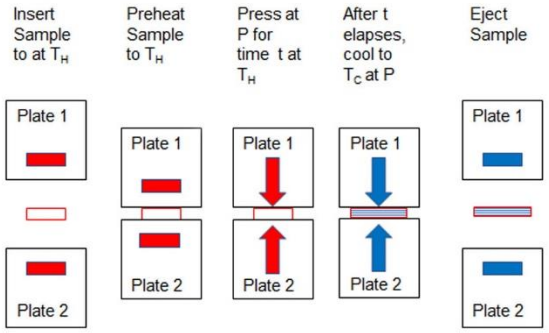

Fig. 8. Hot-pressing procedure and variables
P [Pressure] : 20,000lbs
T_H [Heating Temperature]: 105°C, 115°C, 125°C, 135°C
T_C [Cooling Temperature]: 85°C
t [Time Elapsed]: 10s, 10m, 60m

desired temperature (105°C, 115°C, 125°C, or 135°C) before placing the plates on the press; the press was then closed such that the top clamp contacted the top steel plate without exerting pressure to allow bidirectional heating of the plates and sample for 10 minutes. After that time, 20,000 lb of pressure was applied, taking 16 seconds to reach top pressure. The elevated heat and pressure were maintained for a specified period (10s, 10m, or 60m), before the cooling mechanism was activated. Samples were then cooled to 85°C using a water mediated cooling system while maintaining the 20,000 lb of pressure. The cooling rate was variable and increased in rate with time. The average rate of cooling from the hot-pressing temperature to 100°C and from 100°C to 85°C is detailed in **Table S1**. All cooling rates were relatively slow, never exceeding 0.40°C/min. Three samples were pressed in each time and temperature combination, for a total of 36 samples. Samples were then visualized by placing them between cross-polarized films in order to qualitatively determine if birefringence is present. Two of the three samples pressed at each temperature and time set were subject to thermal and XRD analysis while the other was reserved for future experimentation on how the observed properties change over time.

Thermal Analysis

TMDSC was performed using a Perkin Elmer DSC 7 which was calibrated with a pure indium standard at a heating rate of 10 °C/min. When observed under cross-polarized films, most samples exhibited visually discrete center, middle, and periphery regions; 3-7 mg pieces were analyzed from each region of each sample tested. The TMDSC used a StepScan heating program running from 25°C to 205°C with a heating rate of 5 °C/min, a step size of 2°C, the criteria parameter set to 0.05, and a 1.1 – 1.2 second time resolution between points. The reversing and non-reversing curves were calculated using the Pyris software

X-Ray Diffraction Analysis

A Bruket D-8 Advance X-Ray Diffraction system using DaVinci Software, a Cu X-ray tube, and Bruker Vantec-500 Xe-CO_2 gas filled detector was used to perform XRD and hot-stage XRD. The X-ray operated at 40 kV and 40 mA, and the system optics consisting of a polycap with an output beam divergence of 0.25° and a spot diameter smaller than 4.0 mm. Scans were run with 2θ ranging from 10° - 90°, with scanning times of 60s per step. The scan results were analyzed at a virtual step size of 0.02° and analyzed using the Bruker Diffract-Eva software package (Bruker, Billerica, Massachusetts). For hot stage XRD scans, the sample was heated to the desired temperature using a Bruker TC-DOME Modular Temperature Stage and maintained at the temperature for 5 minutes prior to scanning.

The center, middle, and periphery regions of each examined sample – as previously determined by birefringence analysis – were visualized by XRD. For hot-stage XRD, the center and middle positions of a single 10m sample from each temperature and time combination were

visualized. Hot-stage XRD was performed at 75°C, 100°C, 110°C, 120°C, 170°C, and 220°C; some samples were selected to cool to 25°C after being heated to 220°C, equilibrate for 5 minutes, and then scanned again.

Results and Discussion

Birefringence Analysis:

Hot-pressed samples, as well as unpressed controls, were examined using cross-polarized films to qualitatively discern the presence of birefringence and whether it varies with distance from the sample edge. Samples processed at 105°C, such as those shown in **Figure 9**, show more birefringence at the periphery with increased pressing time, but also largely retain pre-pressing surface features such as marks where spurs were removed and the residual pattern from the sample mold. Samples processed at 115°C for 10s and 10m also retain some surface texture and periphery birefringence; 115°C samples hot-pressed for 1 hour did not retain pre-processing surface features and have comparatively more birefringent area as well as a less optically active center region (**Figure 10**). 125°C samples hot-pressed for 10s show qualitatively similar morphologies to 115°C 60min and 135°C 10s samples. 125 and 135°C samples processed for 10min and 60min increasingly isolate birefringent regions to a halo directly outside the "center" region with decreased optical anisotropy on the periphery (**Figures 11-12**). In addition, at the higher temperatures and time periods, the samples become increasing thin and adhere to the polished stainless-steel plates, making the samples very challenging to remove. Unpressed samples observed under crossed polarized light show almost no optical activity. A limited number of the unpressed samples show very faint birefringence at the edge of the sample (**Figure S1**). This feature can likely be attributed to a meniscus effect during sample preparation: under elevated temperatures when aPS flow occurs, the polymer can adhere to and creep up portions of the mold's walls which likely has the effect of weak hot drawing at the periphery which is then frozen into the sample during the cooling process. However, because of the

comparatively weak optical activity, the limited number of samples effected, and the localization of the effect to small portions on the sample edge, this likely did not play a significant role in the anisotropic properties of the hot-pressed samples.

From strictly qualitative assessments, maximum birefringence was observed in samples hot-pressed at 115°C for 60min and at 125°C for 10s and at 135°C for 10s and 10min. This optical activity may be the result of increased morphological order in the bulk polymer. If the optical anisotropy is due to an increase in order, it may be similar to the birefringence observed in mechanically stretched "frozen-stress" aPS.[3] The birefringence presented here has persisted without obvious change for as long as four months.

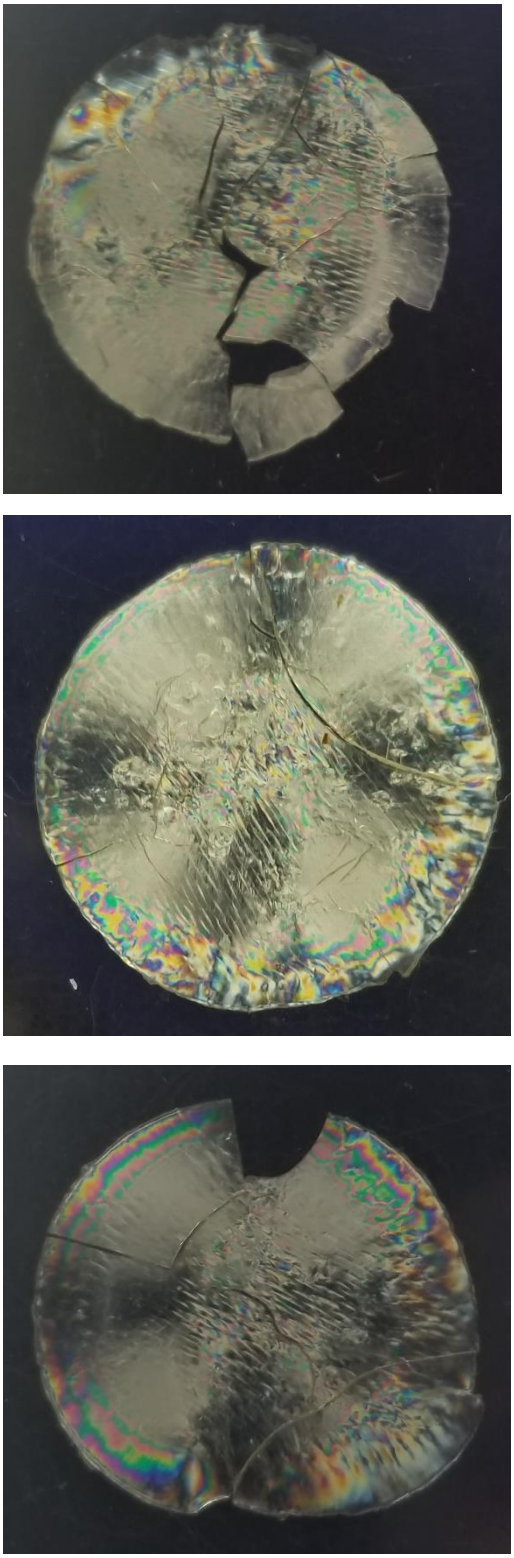

Fig. 9 Samples photographed through cross polarized films to show birefringence. 105°C samples pressed for (top) 10s, (middle) 10min, (bottom) 60min.

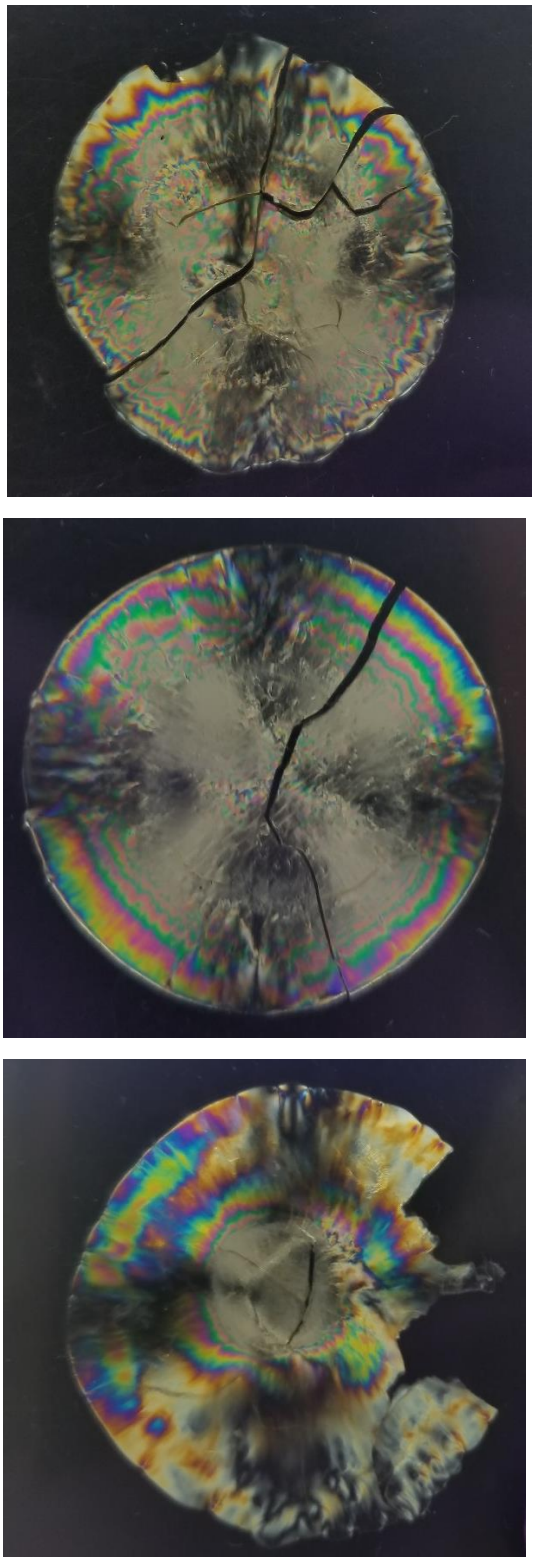

Fig. 10. Samples photographed through cross polaried films to show birefringence. 115°C samples pressed for (top) 10s, (middle) 10min, and (bottom) 60min

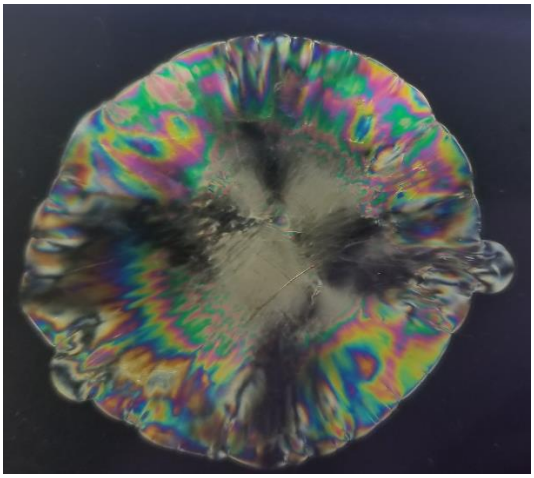

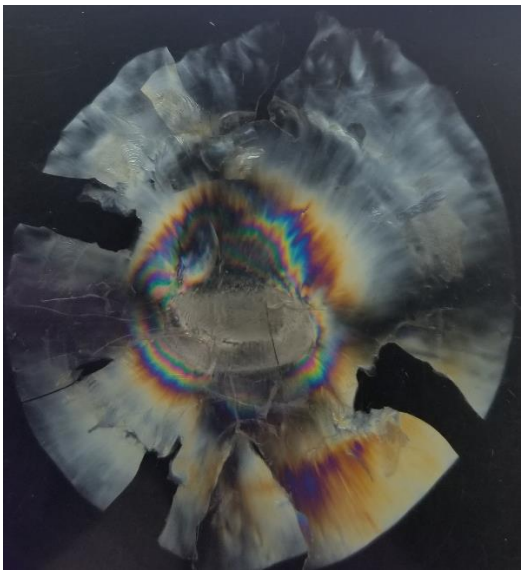

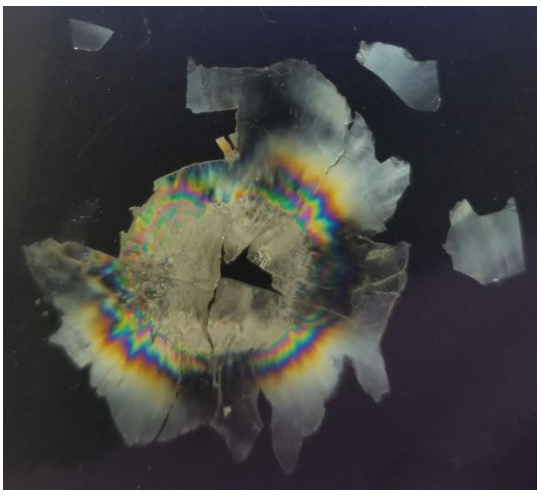

Fig. 11. Samples photographed through cross polarized films to show birefringence. 125°C samples pressed for (top) 10s, (middle) 10min, (bottom) 60min.

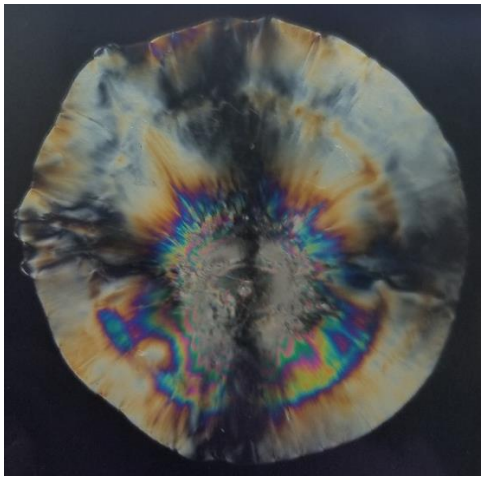

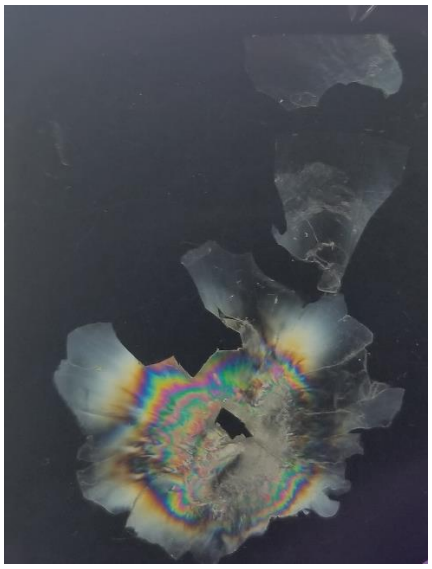

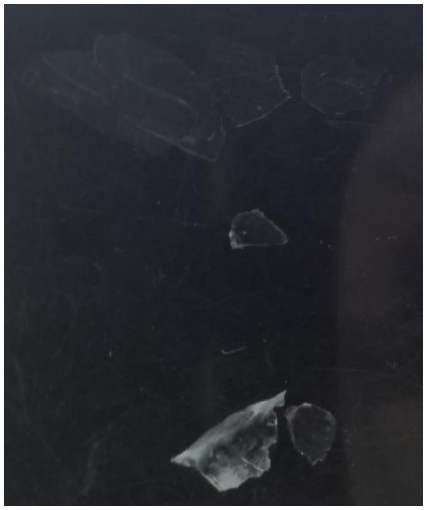

Fig. 12. Samples photographed through cross polaried films to show birefringence. 135°C samples pressed for (top) 10s, (middle) 10min, and (bottom) 60min

Thermal Analysis:

The thermal properties of hot-pressed aPS and control samples were investigated using TMDSC. Since each pressed sample exhibits roughly 3 distinct optical patterns under cross-polarized light, center, middle, and periphery regions from each pressed sample were tested. The reversing and non-reversing curves for each sample were calculated and compared to the batch control samples which experienced identical baking conditions but were not processed.

An investigation of the T_g sought to determine whether the increase observed during compression of aPS is retained in cooled samples. The unpressed control samples have an average T_g = 102.63°C with a standard deviation of 1.01°C. This is slightly lower than many of the literature values for aPS, but within an acceptable range given the distribution of molecular weights in the starting material. Of the 36 sample subsets (3 time periods x 4 temperatures x 3 sample regions), five had the T_g of both samples increase or decrease by at least one standard deviation (1.01°C) from their respective controls. The center region of samples hot-pressed at 115°C for 10 min and the periphery region of samples processed at 105°C for 10 min showed a decrease in T_g by at least 1 standard deviation. For the periphery samples processed at 125°C for 10s and 10m, T_g increased by at least 1 standard deviation; the center regions of samples hot-pressed at 125°C for 10s had T_g increase by at least two standard deviations. The limited changes in T_g as well as the irregularity of the changes does not support the hypothesis that hot-pressing changes the glass transition of aPS. The most likely explanation for this observation is that while compression reduces the v_f of aPS, the combination of elevated pressure and temperature does not induce morphological changes that maximize the attractive forces between aPS chains that would maintain an elevated T_g once pressure is released.

The second goal of studying the thermal transitions of hot-pressed aPS is to observe any transitions related to the specific heat of the material on the reversing curve, or slower kinetically controlled transitions found on the non-reversing curve. The non-reversing curve and the derivative of the non-reversing curve (data not shown) were calculated for all hot-pressed samples and controls. No peaks were observed on any of the non-reversing curves. Derivatives of the non-reversing curves showed that the slope of the non-reversing curve changed during moderate thermal transitions observed on the reversing curve but stayed within 0.32 and 0.44 mW/min. Two potential explanations are presented here. One is that the samples do not exhibit any of the slower thermal transitions associated with the kinetic curve. It is also possible that these transitions occurred but were not detected. A heating rate of 5.0°C/min was used in all TMDSC procedures; this is slower than the 10°C/min rate used in similar studies, but still within the recommended heating range.[9,10,23] It is feasible that the slower heating rate allowed enough time for kinetic transitions to occur during the heating phase, making them unobservable during the holding phase. A heating rate of 10°C/min was considered during preliminary experiments but ultimately not used because it did not produce the approximately sinusoidal heating profile desired in for TMDSC.

Thermal analysis of reverse heat flow data likewise provided inconclusive evidence regarding the presence of mesophases. Of the 12 control samples analyzed, 4 exhibited relatively large endotherm peaks that are not expected in unprocessed aPS. The samples, shown in **Figure S2** with peak statistics detailed in **Table S2**, displayed broad endotherms that appear to consist of two overlapping peaks and span over 13°C temperature intervals at different positions. Hot-pressed samples were directly compared to unpressed controls from each batch as opposed to

aggregate control statistics in order to account for batch to batch variabilities in both thermal and XRD analysis.

In addition to incongruities observed in some unpressed controls, very few of the hot-pressed samples provided comparable thermal transitions data for the center, middle, and periphery regions within a temperature and time subset. A more comprehensive summary of the data is included in the supplementary information (**Figures S3-S14**). Many of the samples' reverse heat flow curves showed thermal transitions, both endothermic and exothermic, in the 175 - 205°C temperature range. Almost all these signals display the double-peak configuration. They vary in absolute energy change from 1.1 to 6.1 mJ, typically residing on the lower end of that range. However, they do not appear with a high enough regularity to draw strong conclusions.

X-ray Diffraction Analysis

The XRD measurements were unable to directly observe electron density associated with the aPS backbone due to instrument limitations. However, the activity of the polymer backbone can be at least partially inferred by analyzing the styrene peak. Hot-pressed samples with the most birefringence when observed via cross-polarized films tend to also have the greatest increase in the styrene peak height, which is associated with increased stacking of the styrene side groups compared to unpressed controls.

Hot stage XRD is used to interrogate the temperature-dependence of the styrene peak in aPS. Control samples were examined by hot stage XRD, as shown in **Figures 13 and S15**. In these cases, the sample had comparable peak shape from 75 – 120°C and decreased in height at

170°C. This behavior likely occurs because even though the polymer backbone is more labile and expanded under increased temperatures – enlarging the inter-chain peak – there was no bulk flow that would induce superchain alignment and encourage side group stacking, as shown in **Figure 14**.[22] At 170°C and 220°C the high temperatures likely thermally disorders the side chains and backbone, hindering alignment.

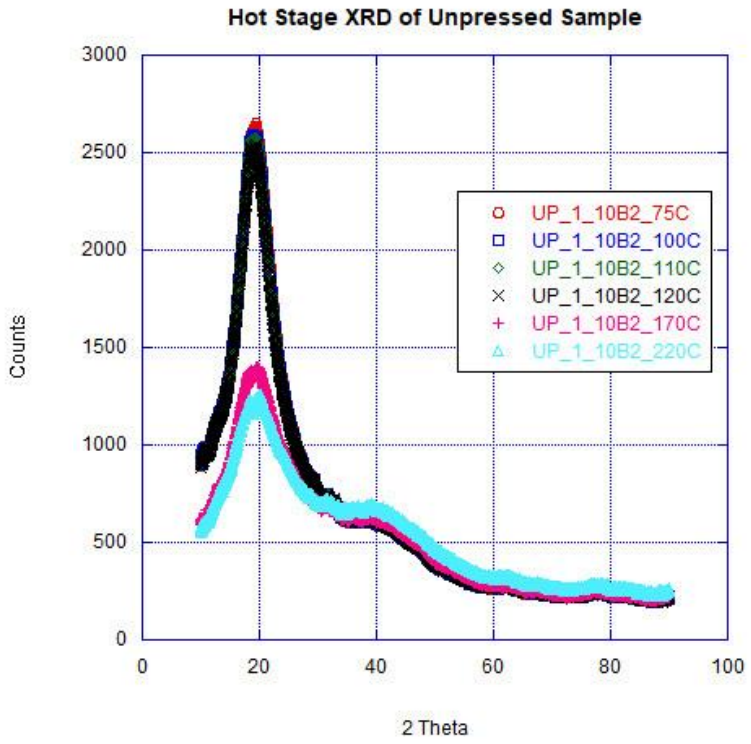

Fig. 13. Hot stage XRD of unpressed aPS with scans taken at 75°C (red), 100°C (blue), 110°C (green), 120°C (black), 170°C (pink), and 220°C (light blue). 75°C - 110°C curves obscured by 120°C curve.

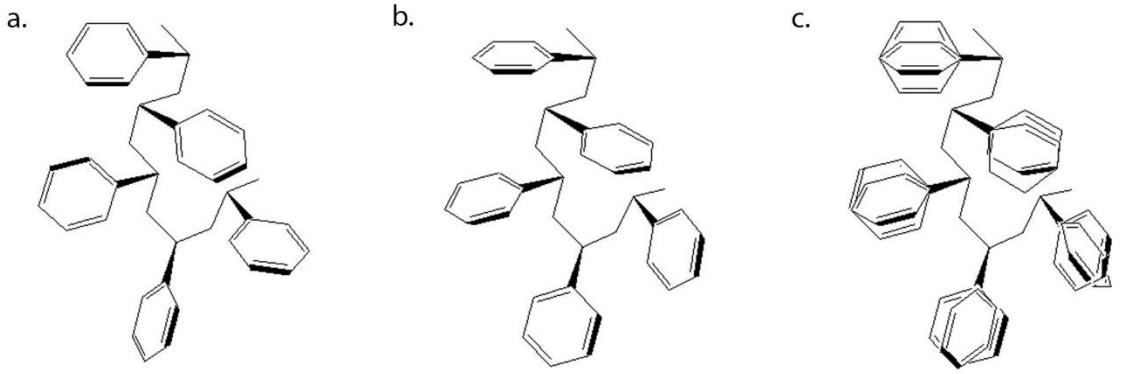

Fig. 14. Unpressed aPS morphology observed by hot stage XRD under **(a)** 75 - 110°C where not enough energy for the styrene groups to rotate **(b)** 120°C where styrene groups can rotate but cannot stack due to superchain disorder **(c)** 170 - 220°C where thermal disorder decreases the XRD signal of the styrene peak

For the samples hot-pressed at 135°C, shown in **Figures 15 and S16**, the styrene peak is the same from 75 - 110°C and increases at 120°C before decreasing at temperatures above 170°C. The increase in the styrene peak observed at 120°C in hot-pressed samples compared to the controls suggests that flow-induced superchain alignment encourages side group stacking once they have enough energy to rotate. It is hypothesized that between 110°C and 120°C, some percentage of the phenyl side groups gain enough energy to rotate and reach a more energetically favorable oriented stacking conformation, but alignment of the polymer backbone is a prerequisite. No peaks were observed in the non-reversing curve of the TMDSC, but investigation using different program parameters may visualize this transition in future experiments. The large decrease in peak intensity at 170°C confirms the role of thermal disorder on the styrene peak. When the sample is cooled back to 25°C, it maintains the disorder relative to the sample at 75°C. The thermal transitions are further illustrated in **Figure 16**. This suggests

that the intensity of the styrene peak prior to thermal disorder is a result of the hot-pressing technique rather than a property inherent to the material itself.

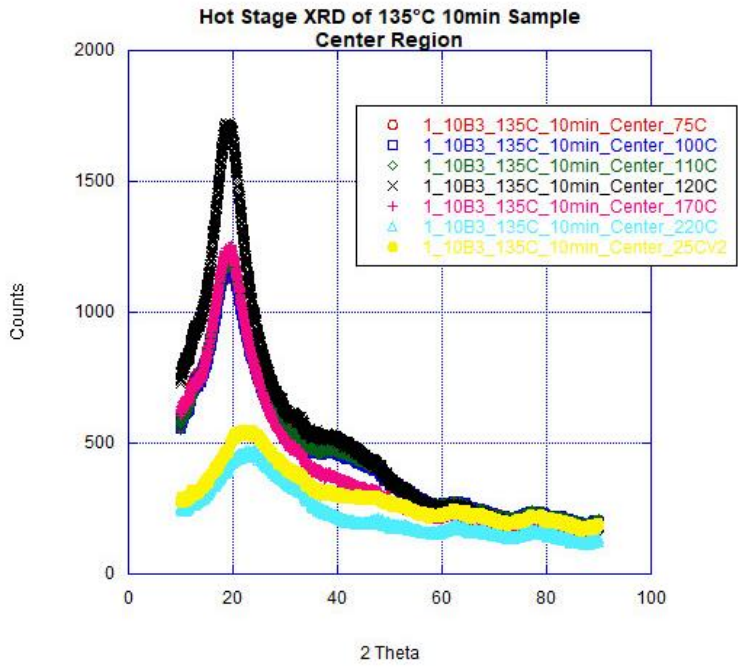

Fig. 15. Hot stage XRD scans of the center region of aPS hot pressed at 135°C for 10min, with scans at 75°C (red), 100°C (blue), 110°C (green), 120°C (black), 170°C (pink), 220°C (light blue), and then after the sample cooled to 25°C (yellow). Data from 75°C - 110°C and 170°C approximately concurrent, obscuring peaks.

Samples hot-pressed at 105, 115, and 125°C, as seen in **Figures S17-S19**, exhibit irregular behavior under hot stage XRD that raise questions over how different regions of the sample experience the processing technique. In all three cases, the center samples exhibit the expected transitions with the styrene peak intensifying at 120°C before decreasing at 170°C. In contrast, the middle regions showed intensification of the styrene peak through 170°C, and in some cases through 220°C. One potential explanation is that at lower hot-pressing temperatures, differences in the flow patterns of the center and middle regions become more pronounced, leading to morphologies that result in side chain reorganization at higher temperatures. A more

detailed investigation of the mechanism by which hot pressing results in radially varied morphologies is warranted.

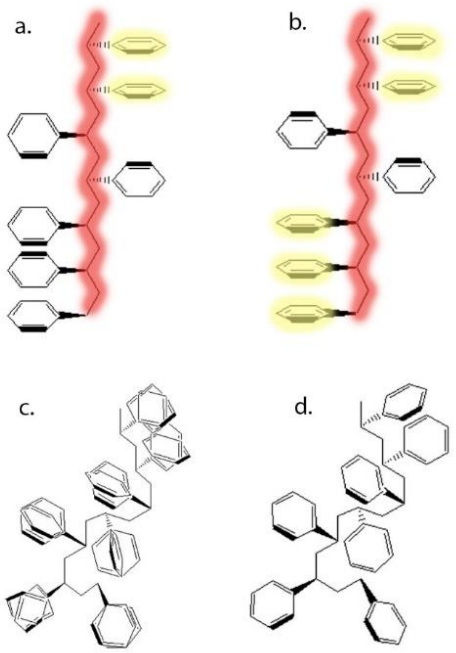

Fig. 16. aPS hot-pressed at 135°C for 10 minutes examined by hot stage XRD at **(a)** 75 - 110°C, where insufficient thermal energy for styrene rotation **(b)** 120°C, where styrene groups likely have enough energy to rotate and adopt the stacking configuration **(c)** 170 - 220°C where thermal disorder lowers the styrene peak **(d)** upon cooling to 25°C where the thermal disorder is retained because of no mechanical alignment during heating.

All scanned samples hot-pressed at 135°C for 10s and 10m and at 125°C for 10s display large increases in the intensity of the styrene peak at room temperature compared to unpressed controls, as shown in **Figures 17-19** and **S27, S29-S30**. This increase in the styrene peak is likely due to an alignment of parts of the aPS superchain during the hot-pressing process, which would in turn increase the number of irregular phenyl stacks resulting in a more intense characteristic peak at 19°.[22] Smaller increases in peak intensity were also observed in samples hot-pressed at 105 and 115°C for 10s, as shown in **Figures S20-S26**. The disparity in peak intensification between low and high processing temperatures suggests that higher processing temperatures

allow for more superchain mobility, and the sample is therefore more easily aligned. It is also possible that below 120°C, the superchain can align, resulting in birefringence, but the phenyl side groups are unable to adopt a more stable stacking conformation. That would partially explain why the samples hot-pressed at 115°C showed significant amounts of optical anisotropy but no increase in the styrene peak compared to controls. A quantitative approach to measuring the birefringence would determine whether the samples hot-pressed below 125°C showed only positive birefringence, indicating chain alignment but no side group stacking.

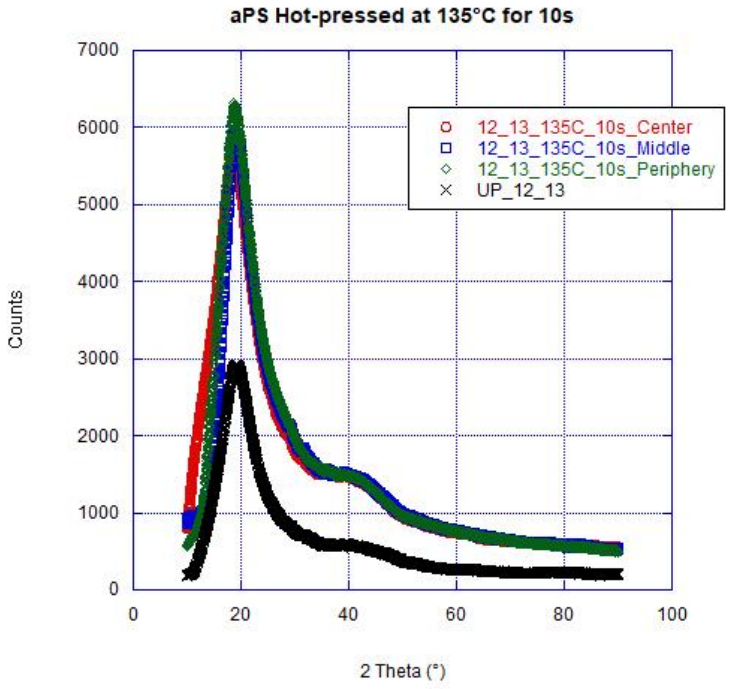

Fig. 17. XRD scans of center (red), middle (blue), and periphery (green) regions of aPS sample hot-pressed at 135°C for 10s compared to unpressed control (black).

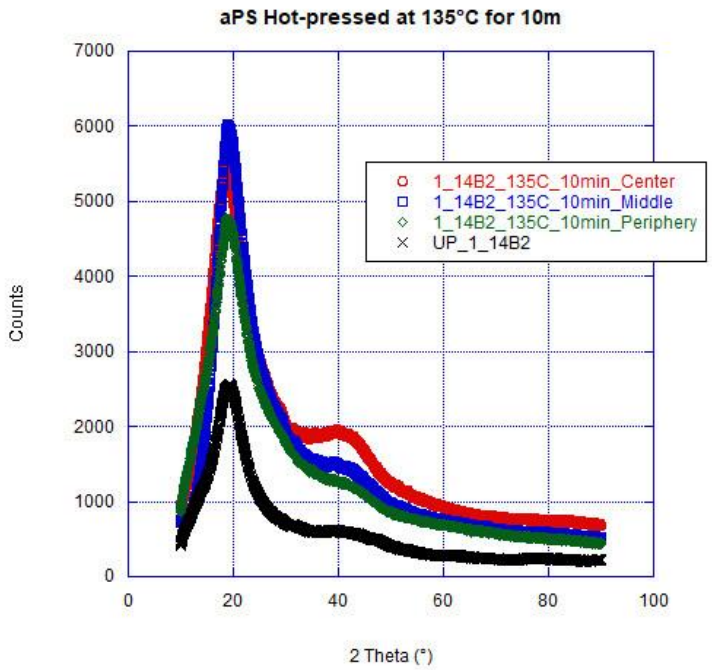

Fig. 18. XRD scans of center (red), middle (blue), and periphery (green) regions of aPS sample hot-pressed at 135°C for 10min compared to unpressed control (black).

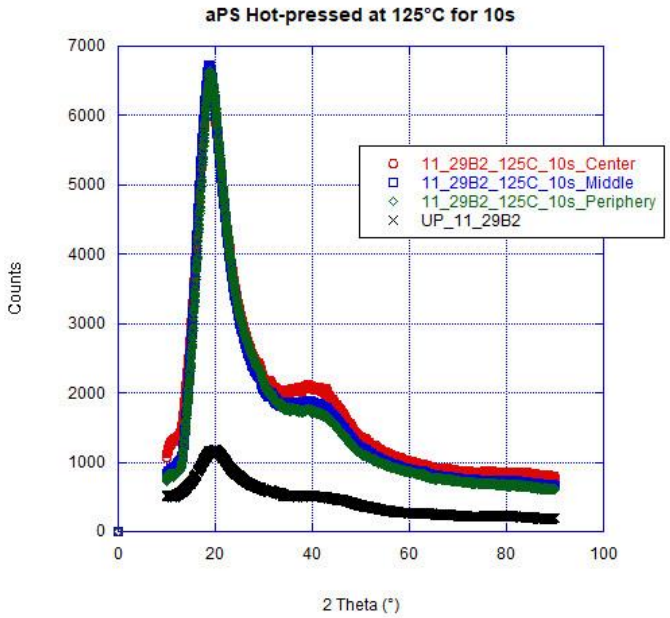

Fig. 19. XRD scans of center (red), middle (blue), and periphery (green) regions of aPS sample hot-pressed at 125°C for 10s compared to unpressed control (black).

In addition to temperature, the length of time for hot-pressing appears to contribute to the intensification of the XRD styrene peak which suggests the alignment process may have kinetic and equilibrium-mediated components. 125°C, and 135°C samples hot-pressed for 60m consistently showed a decrease in the styrene peak, as shown in **Figures 20, S28, and S31**. Possible explanations for this behavior include that given enough time, the aPS backbone will adopt a more stable and less linear structure, or the side groups will shift to a more stable conformation with less stacking. Another potential explanation is that the 60m samples are the thinnest for each temperature profile, meaning that there are fewer opportunities for the incident X-Ray beam to interact with the sample.[25] No evidence is presented here to favor one explanation or the other, but the potential influence of these factors may partially explain the heterogenous mix of increase and decreases in the styrene peaks observed in 10 min (excluding those processed at 135°C) and 60min samples.

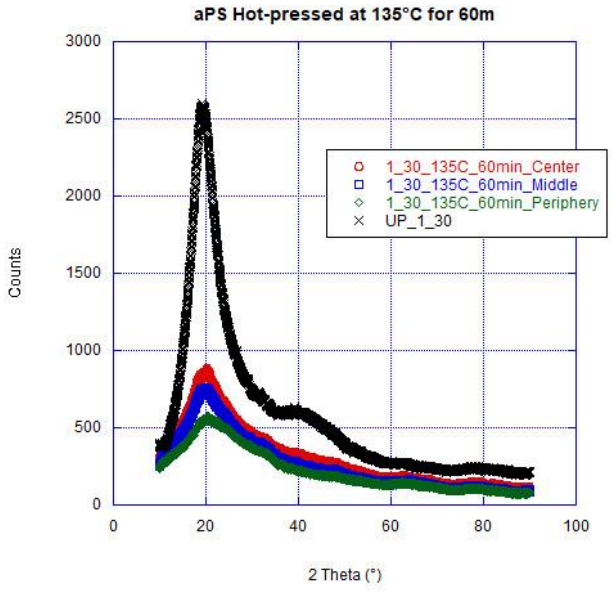

Fig. 20. XRD scans of center (red), middle (blue), and periphery (green) regions of aPS sample hot-pressed at 135°C for 60min compared to unpressed control (black).

Conclusions:

The optical anisotropy induced by hot-pressing aPS appears both dependent on the temperature and duration of the procedure with the samples processed at 125°C for 10s and 135°C for 10s and 10m showing stronger styrene peaks when observed by XRD. This behavior likely indicates that hot-pressing under these conditions aligns the aPS superchain in a way that allows for limited stacking of the randomly distributed phenyl side groups, a process that has been observed via birefringence and XRD measurements of heated and mechanically stretched aPS.[5-8,21,22] A quantitative approach to measuring this would likely confirm that the samples adopt negative birefringence. Samples processed below 125°C likewise have birefringent properties but lack the corresponding intensification of the styrene peak. This likely corresponds to an alignment of the aPS backbone, producing positive birefringence, without enough energy for side group rotation and stacking. Like "frozen stress" mechanically stretched samples, the anisotropy induced by hot-pressing in both cases appears long lived.

Due to equipment limitations, the expected ordering of the 0.75 $Å^{-1}$ interchain peak associated with the aPS backbone was unobserved. Further experimentation is warranted to confirm the predictions from this study. At smaller 2 theta angles (< 10°), an increase in peak intensity compared to unpressed controls is expected for all samples exhibiting birefringence.

The lack of thermal evidence supporting the theory of superchain alignment frustrates this analysis. As previously stated, it is possible that the slow rate of heating during the reversing curve may have allowed kinetically controlled processes time to equilibrate outside the non-reversing phase. Another potential explanation is that the process of hot-pressing engenders mechanical defects in aPS such as crazes and microvoids. Mechanical stresses that induce these

defects frequently result in chain scission, which would complicate the DSC readings with more low molecular weight byproducts as well as contribute to the optical anisotropy.[4] Gel permeation chromatography could be used to determine whether hot-pressing results in the production of more low molecular weight polymer fragments.

The evidence presented supports the hypothesis that a stable mesophase, very similar to that reported for "frozen stress" mechanically stretched polymers, is induced in aPS through hot-pressing. Future research closely comparing the products of the processes can now be undertaken to examine the different mechanical properties, especially tensile strength. Additionally, these experiments add to the body of research on aPS photoelasticity and on hot-pressing of polymers, showing that stable optical anisotropy can be induced through compression in an entirely amorphous polymer.

Bibliography:

1. Brazel, Christopher S., and Stephen L. Rosen. *Fundamental Principles of Polymeric Materials.* 3rd ed., John Wiley & Sons, Inc., 2012.
2. Muthukumar, Murugappan. *Progress in Understanding of Polymer Crystallization: Shifting Paradigms in Polymer Crystallization.* Edited by Günter Reiter and Gert R. Strobl, Springer-Verlag Berlin Heidelberg, 2007.
3. Zhang, X., Ajji, A. Biaxial Orientation Behavior of Polystyrene: Orientation and Properties. *J. App. Poly. Sci.* **89,** 487-496 (2003).
4. Callister, W. D., and D. G. Rethwisch. *Callister & Rethwisch.* 9th ed., Pearson Education, Inc., 1974.
5. Nielsen, L. E., Buchdahl, R. Visoelastic and Photoelastic Properties of Polystyrene above Its Softening Temperature. *J. Chem. Phys.* **17,** 839 (1949).
6. Kolsky, H., Shearman, A. C. Photo-elastic investigations of structural changes in plastic materials. *Proc. Phys. Soc.* **55,** 383 (1943).
7. Andrews, R. D., Rudd, J. F. Photoelastic Properties of Polystyrene in the Glassy State. I. Effect of Molecular Orientation. *J. App. Phys.* **28,** 1091 (1957).
8. Rudd, J. F., Gurnee, E. F. Photoelastic Properties of Polystyrene in the Glassy State. II. Effect of Temperature. *J. App. Phys.* **28,** 1096 (1957).
9. Baker, C. M., Azagury, A. & Mathiowitz, E. Effect of pressure on poly-L-Lactic Acid morphology. *Polym. (United Kingdom)* **99,** 250-262 (2016).
10. Baptista, Cameron. *Developments Toward the Characterization and Quantification of Pressure-Temperature Induced Mesophases in Non-Mesogenic Thermoplastic Polymers*. Master's Thesis submitted to Brown University (2018).

11. Sorrentino, A., Santis, F. D., Titomanlio, G. *Progress in Understanding of Polymer Crystallization: Polymer Crystallization Under High Cooling Rate and Pressure: A Step Towards Polymer Processing Conditions.* Edited by Günter Reiter and Gert R. Strobl, Springer-Verlag Berlin Heidelberg, 2007.
12. Höhne, G.W.H. High Pressure differential scanning calorimetry on polymers. *Thermochimica Acta*. **332,** 115-123 (1999).
13. Kojima, Y., Takahara, M., Matsuoka, T., Takahashi, H. High Pressure Differential Thermal Analysis of Polymers. *J. Appl. Pol. Sci.* **80,** 1046-1051 (2001).
14. Angelloz, C., Fulchiron, R., Douillard, A., Chabert, B., Fillit, R., Vautrin, A., David, L. Crystallization of Isotactic Polypropylene under High Pressure (γ Phase). *Macromol.* **33,** 4138-4145 (2000).
15. Stevens, J. R., Coakley, R. W., Chau, K. W., Hunt, J. L. The pressure variation of the glass transition temperature in atactic polystyrene. *J. Chem. Phys.* **84,** 1006 (1986).
16. Strobl, G. From the melt via mesomorphic and granular crystallinity to lamellar crystallites: A major route followed in polymer crystallization. *Eur. Phys. J. E.* **3,** 165-183 (2000).
17. Sirota, E. B. Polymer Crystallization: Metastable Mesophases and Morphology. *Macromol.* **40,** 1043-1048 (2007).
18. Elmoumni, A., Winter, H. H., Waddon, A. J., Fruitwala, H. Correlation of material and processing time scales with structure in isotactic polypropylene crystallization. *Macromol.* **36,** 6453 (2003).
19. Somani, R. H., Yang, L., Hsiao, B. S. Precursors of primary nucleation induced by flow in isotactic polypropylene. *Physica A.* **304,** 145 (2002).

20. Kanaya, T., Takayama, Y., Ogino, Y., Matsuba, G., Nishida, K. *Progress in Understanding of Polymer Crystallization: Precursor of Primary Nucleation in Isotactic Polystyrene Induced by Shear Flow.* Edited by Günter Reiter and Gert R. Strobl, Springer-Verlag Berlin Heidelberg, 2007.
21. Kolsky, H. Stress-Birefringence in Polystyrene. *Nature.* **4214,** 235 (1950).
22. Mitchell, G. R., Windle, A. H. Structure of polystyrene glass. *Polymer* **25,** 906-920 (1984).
23. Simon, S. Temperature-modulated differential scanning calorimetry: theory and application. *Thermo. Acta* **374,** 55-71 (2001).
24. Thomas, L. C. Modulated DSC Paper #1 Why Modulated DSC?; An Overview and Summary of Advantages and Disadvantages Relative to Traditional DSC. *TA Instruments.* (2005).
25. Widjonarko, N. E. Introduction to Advanced X-ray Diffraction Techniques for Polymeric Thin Films. *Coatings* **6,** 54 (2016).

Supplementary Information:

Table S1: Average cooling rates for hot-pressed samples from starting temperature to 100°C

Hot-pressing sample Temperature	135°C	125°C	115°C	105°C
Cooling Rate (°C/min)	0.250	0.178	0.141	0.075

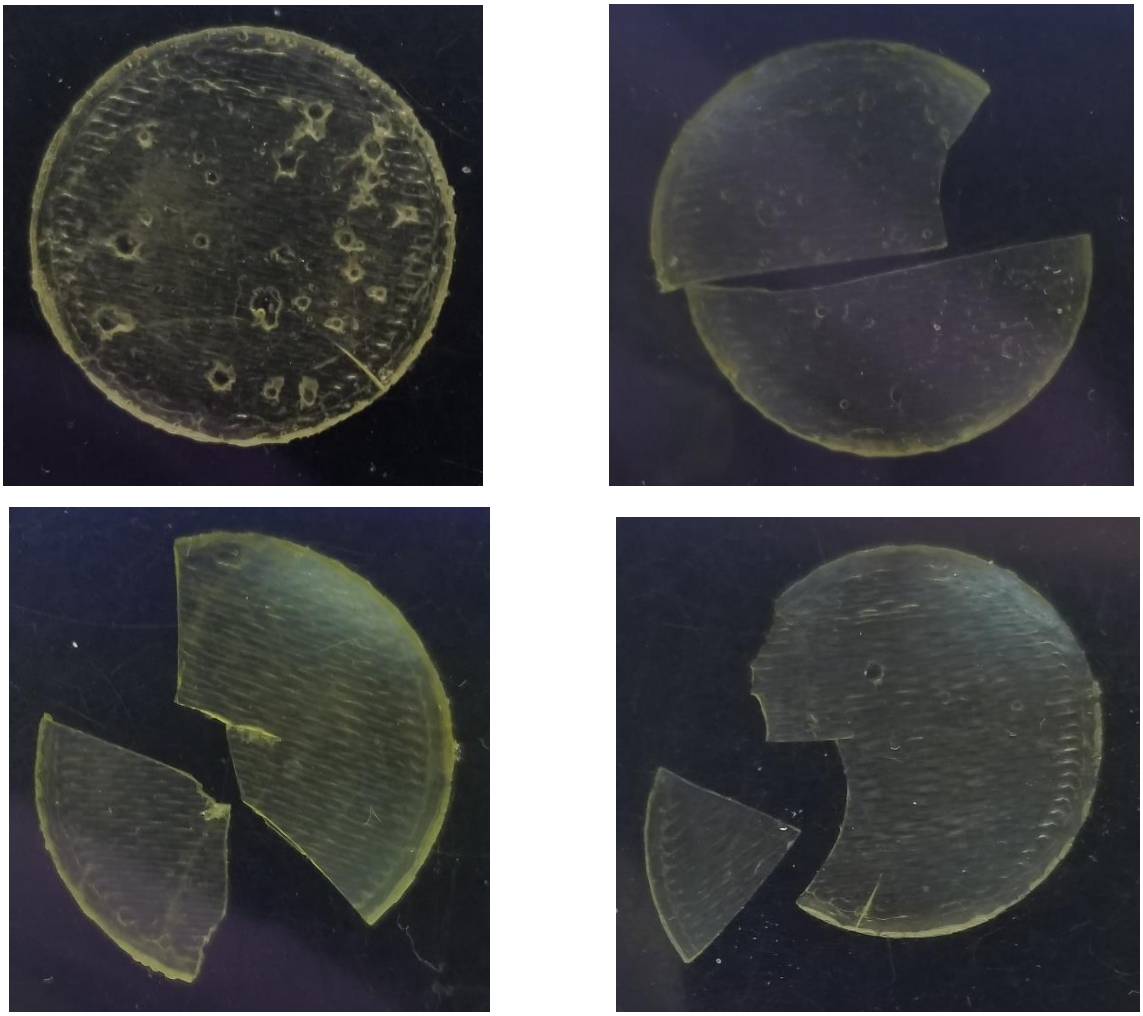

Fig. S1. Unpressed samples photographed through polarized films to show lack of birefringence. Beginning at top left, samplse from batch 1_30, 11_28B2, 11_29B1, 11_29B2.

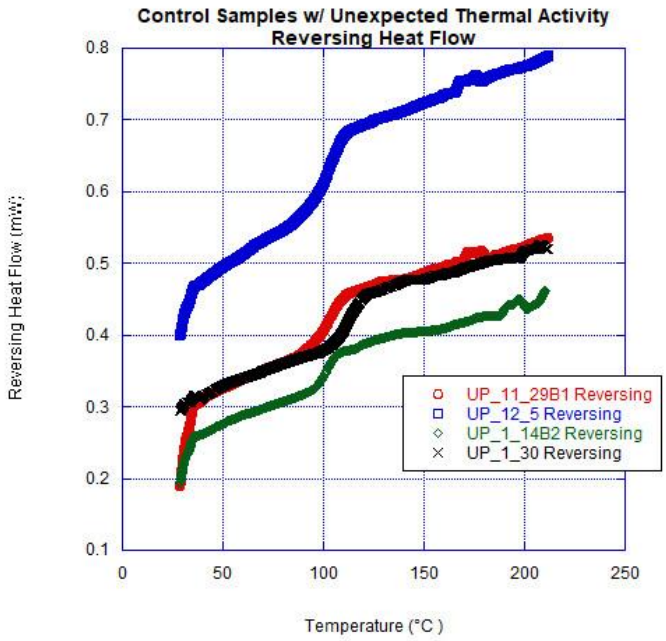

Fig. S2. Reverse heat flow of unpressed samples showing unexplained endotherms.

Table S2: Figure S2 Endotherm statistics.

Sample ID	Temperature Interval (°C)	Peak Area (mJ)	ΔH (J/g)
11_29B1 (red)	169 – 182.5	3.329	0.695
12_5 (blue)	160 – 174	3.125	0.401
1_14B2 (green)	189 – 202.5	3.288	0.862
1_30 (black)	179 – 192	2.055	0.351

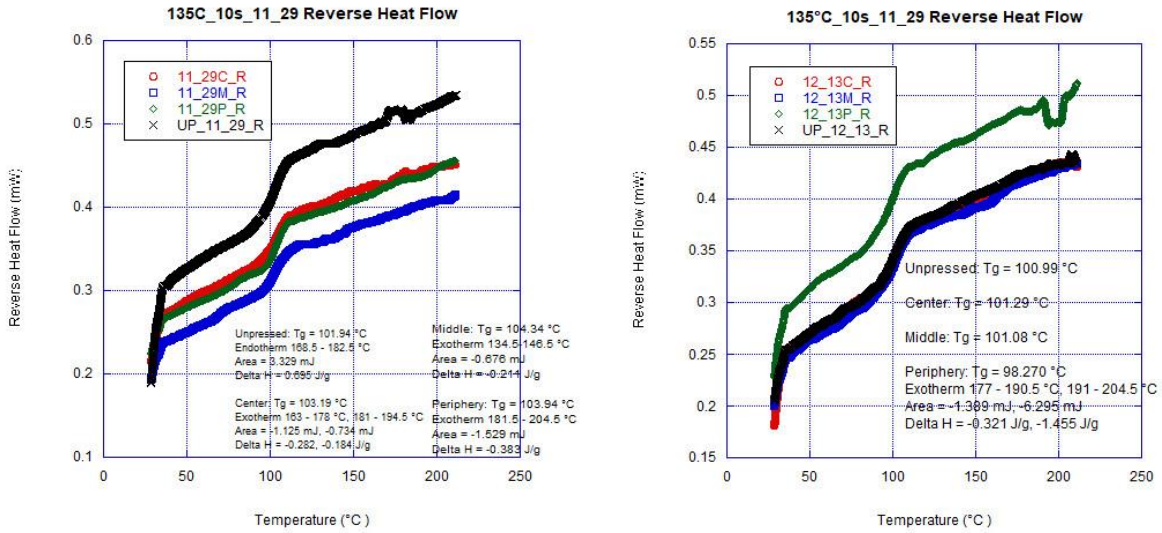

Fig. S3. Reverse heating curves, T_g, and large endo- and exotherms calculated from TMDSC for aPS hot-pressed at 135°C for 10s. Samples from center (red), middle (blue), periphery (green), and unprocessed controls from the same batch (black) were examined.

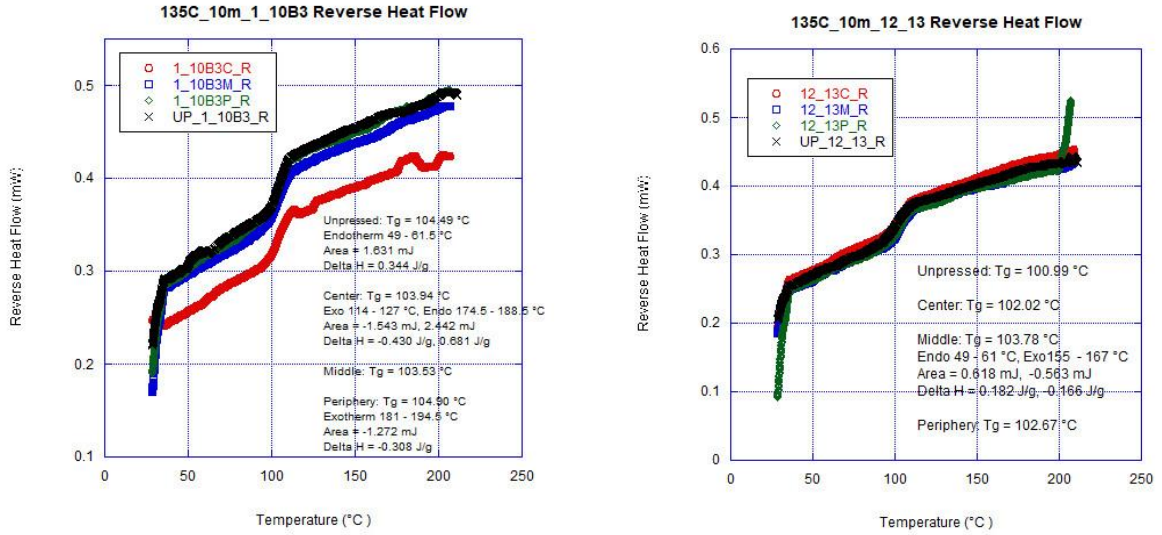

Fig. S4. Reverse heating curves, T_g, and large endo- and exotherms calculated from TMDSC for aPS hot-pressed at 135°C for 10m. Samples from center (red), middle (blue), periphery (green), and unprocessed controls from the same batch (black) were examined.

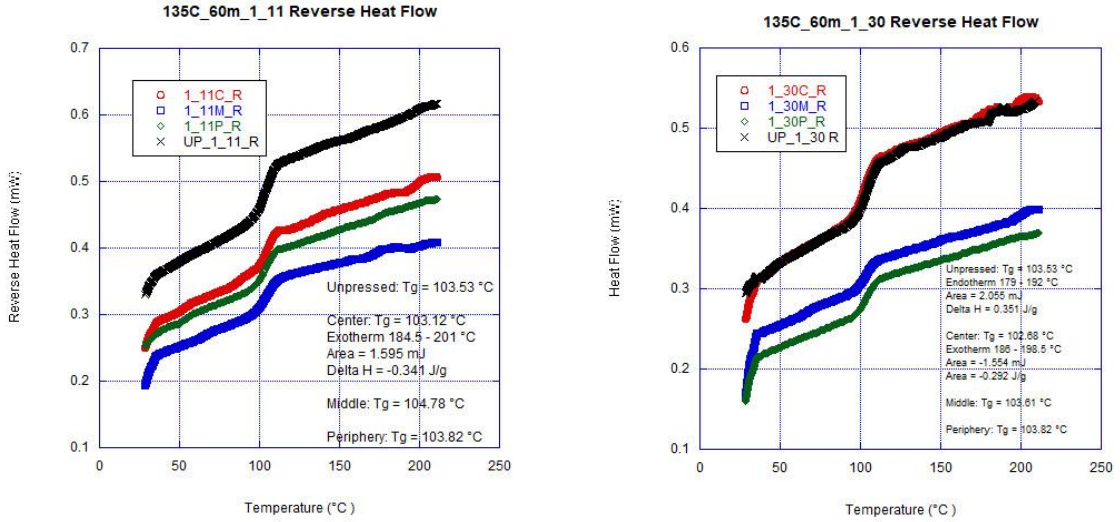

Fig. S5. Reverse heating curves, T_g, and large endo- and exotherms calculated from TMDSC for aPS hot-pressed at 135°C for 60m. Samples from center (red), middle (blue), periphery (green), and unprocessed controls from the same batch (black) were examined.

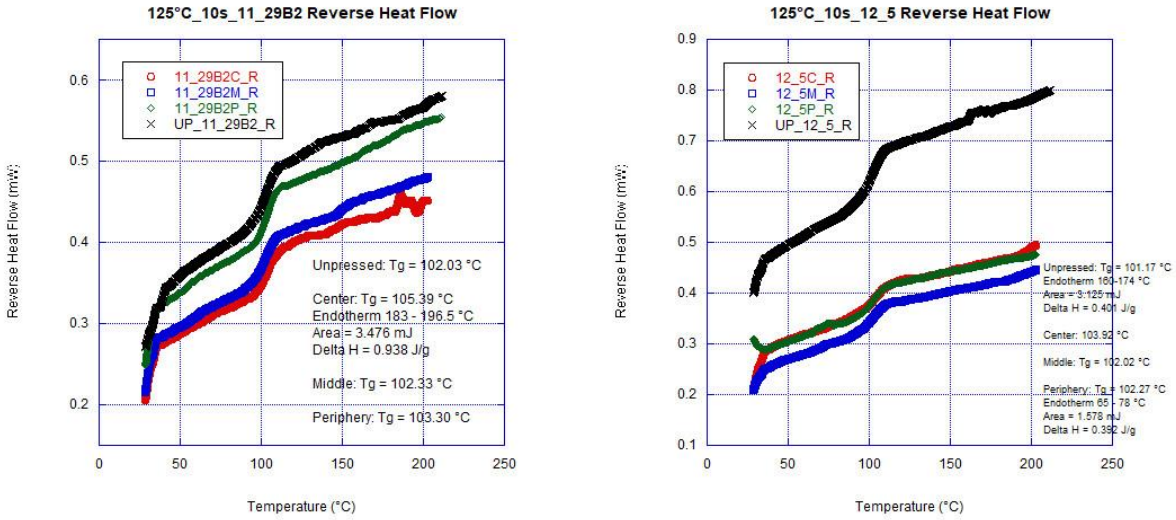

Fig. S6. Reverse heating curves, T_g, and large endo- and exotherms calculated from TMDSC for aPS hot-pressed at 125°C for 10s. Samples from center (red), middle (blue), periphery (green), and unprocessed controls from the same batch (black) were examined.

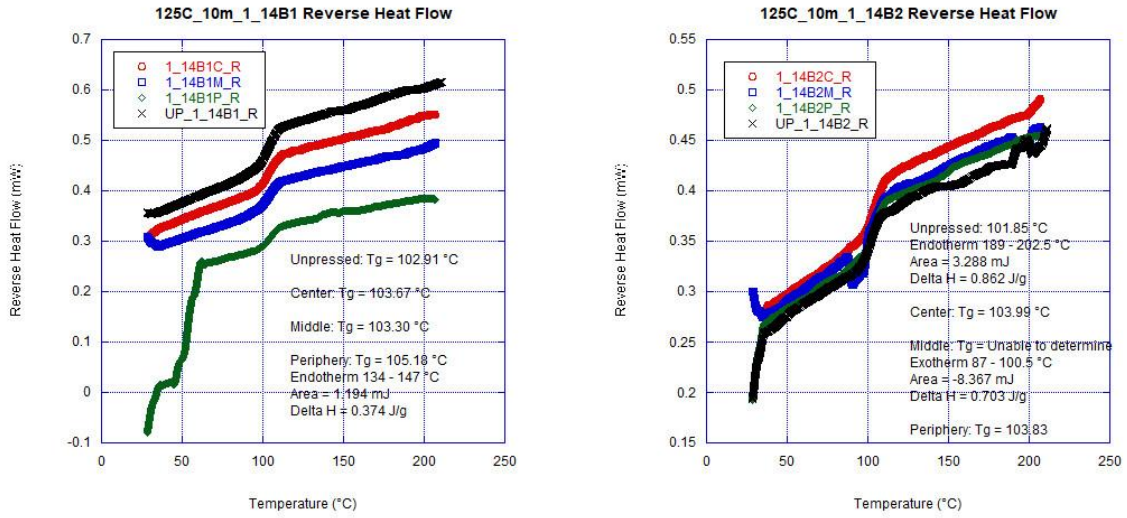

Fig. S7. Reverse heating curves, T_g, and large endo- and exotherms calculated from TMDSC for aPS hot-pressed at 125°C for 10m. Samples from center (red), middle (blue), periphery (green), and unprocessed controls from the same batch (black) were examined.

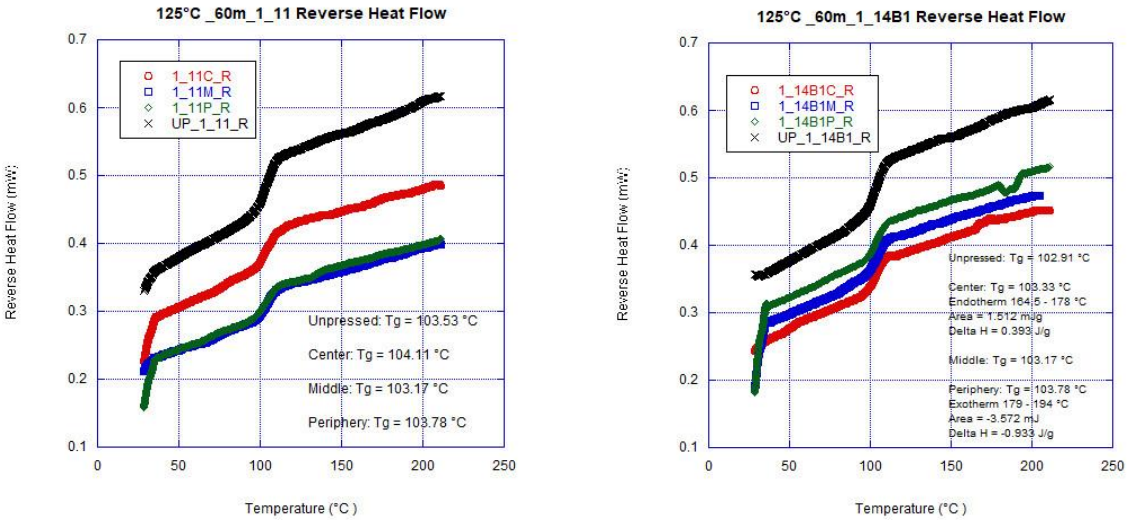

Fig. S8. Reverse heating curves, T_g, and large endo- and exotherms calculated from TMDSC for aPS hot-pressed at 125°C for 60m. Samples from center (red), middle (blue), periphery (green), and unprocessed controls from the same batch (black) were examined.

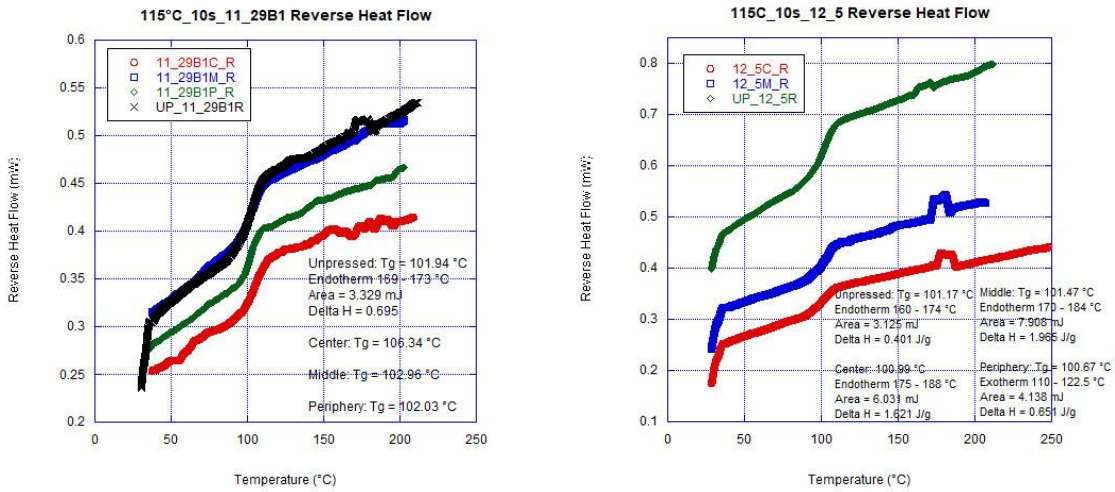

Fig. S9. Reverse heating curves, T_g, and large endo- and exotherms calculated from TMDSC for aPS hot-pressed at 115°C for 10s. Samples from center (red), middle (blue), periphery (not shown), and unprocessed controls from the same batch (green) were examined.

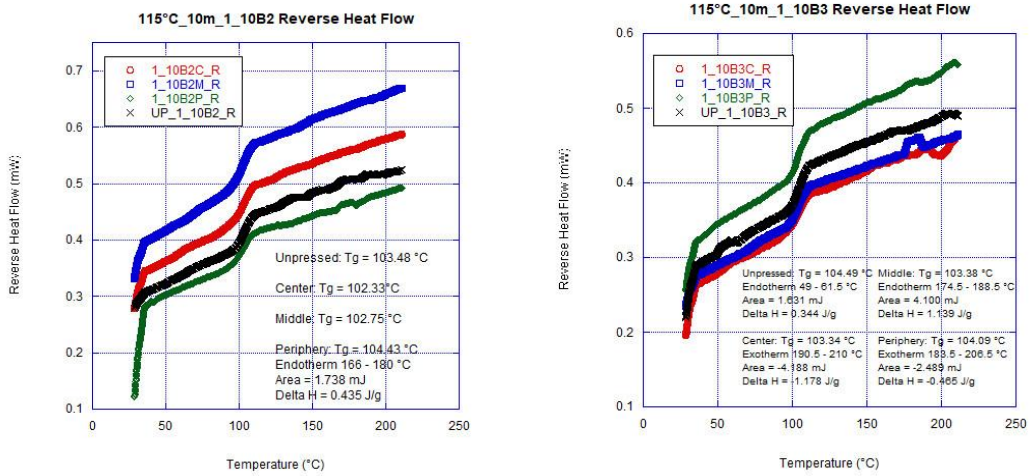

Fig. S10. Reverse heating curves, T_g, and large endo- and exotherms calculated from TMDSC for aPS hot-pressed at 115°C for 10m. Samples from center (red), middle (blue), periphery (green), and unprocessed controls from the same batch (black) were examined.

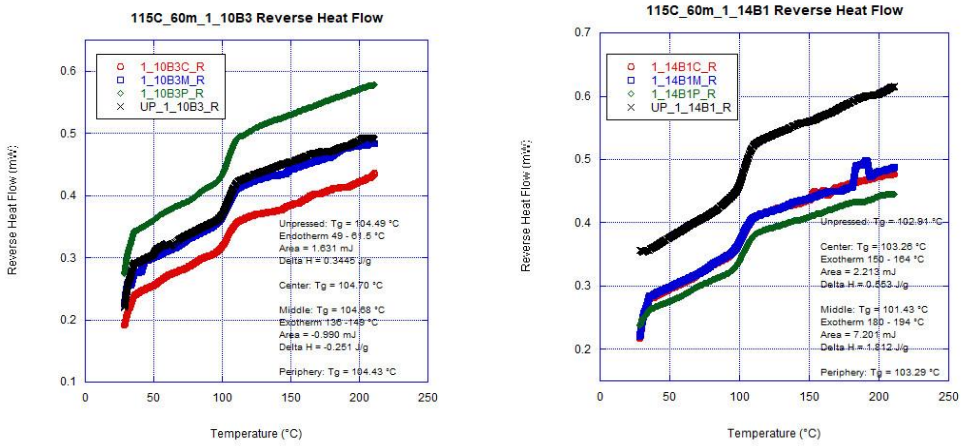

Fig. S11. Reverse heating curves, T_g, and large endo- and exotherms calculated from TMDSC for aPS hot-pressed at 115°C for 60m. Samples from center (red), middle (blue), periphery (green), and unprocessed controls from the same batch (black) were examined.

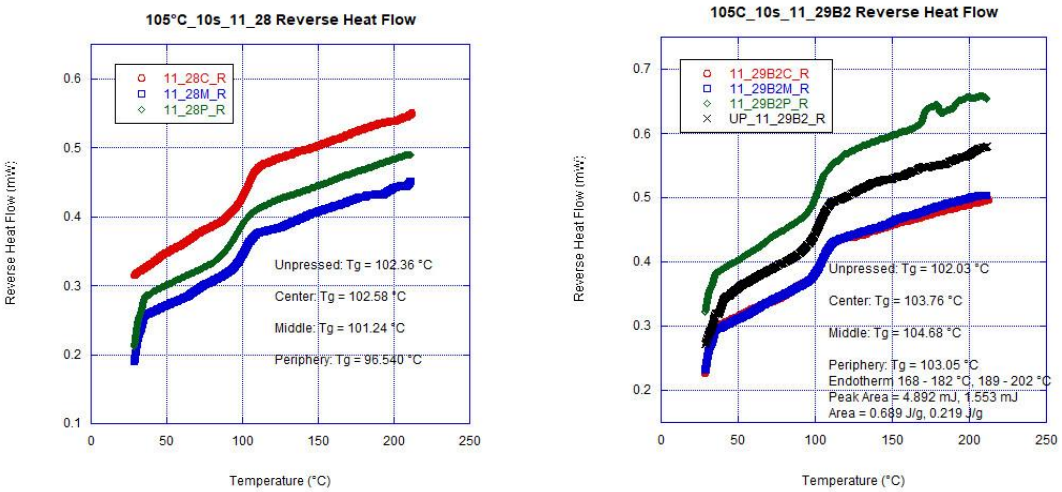

Fig. S12. Reverse heating curves, T_g, and large endo- and exotherms calculated from TMDSC for aPS hot-pressed at 105°C for 10s. Samples from center (red), middle (blue), periphery (green), and unprocessed controls from the same batch (black) were examined.

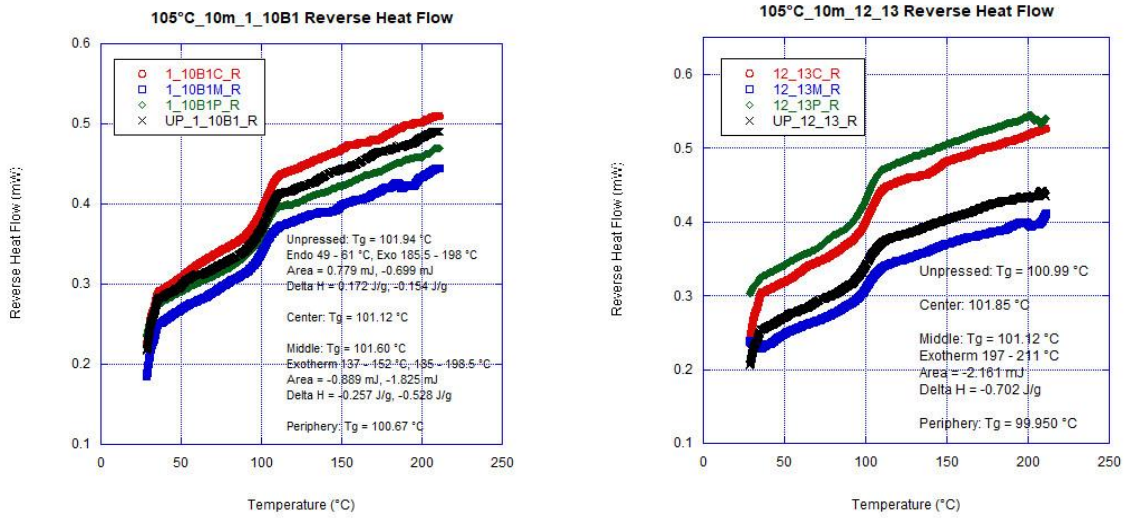

Fig. S13. Reverse heating curves, T_g, and large endo- and exotherms calculated from TMDSC for aPS hot-pressed at 105°C for 10m. Samples from center (red), middle (blue), periphery (green), and unprocessed controls from the same batch (black) were examined.

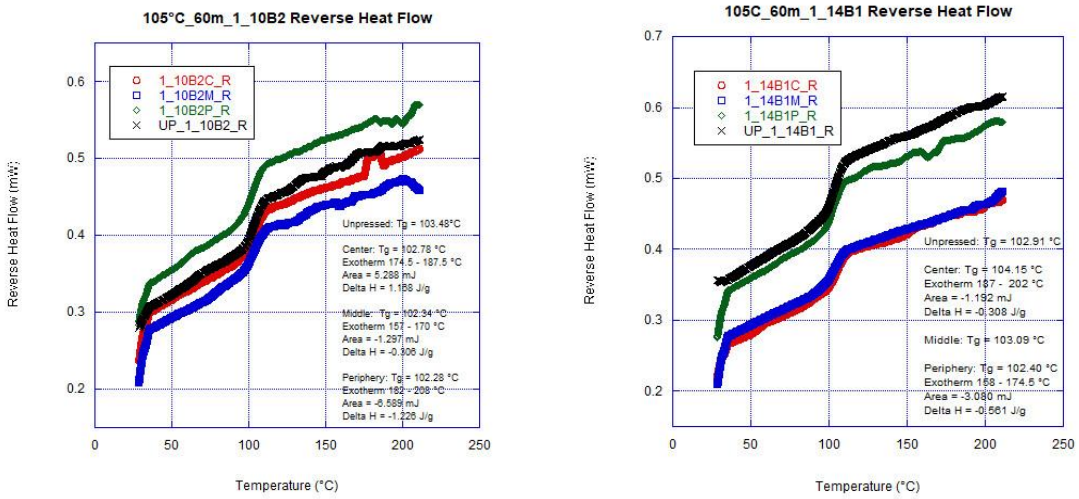

Fig. S14. Reverse heating curves, T_g, and large endo- and exotherms calculated from TMDSC for aPS hot-pressed at 105°C for 60m. Samples from center (red), middle (blue), periphery (green), and unprocessed controls from the same batch (black) were examined.

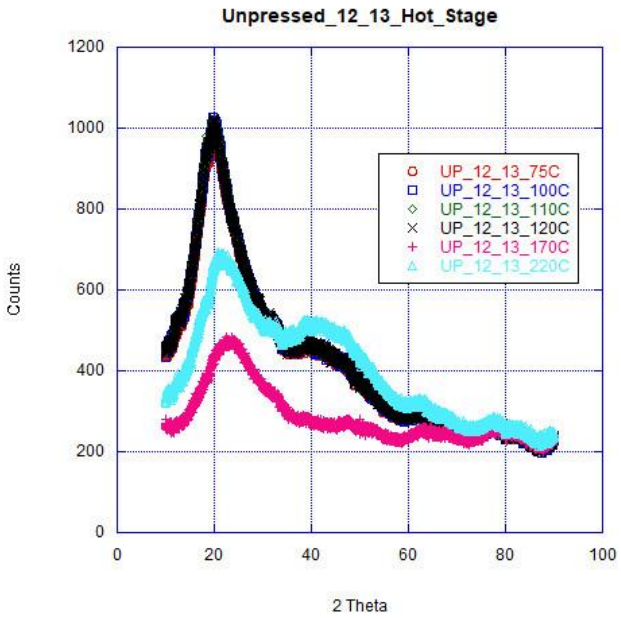

Fig. S15. Hot stage XRD of unpressed aPS with scans taken at 75°C (red), 100°C (blue), 110°C (green), 120°C (black), 170°C (pink), and 220°C (light blue). 75°C - 110°C curves obscured by 120°C curve.

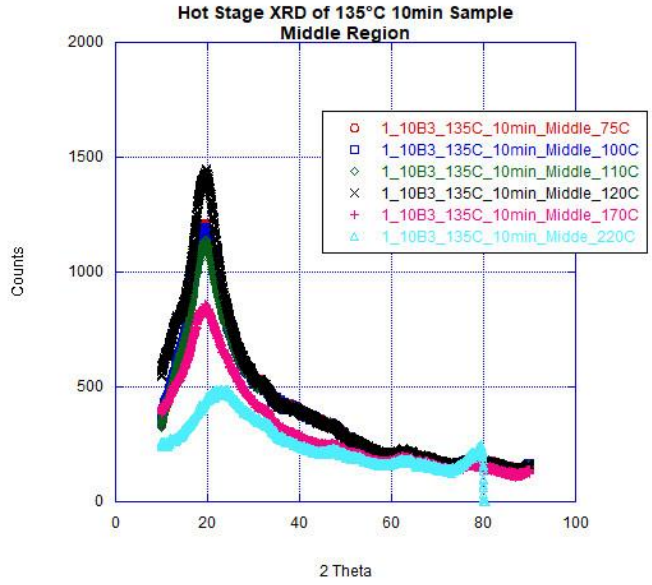

Fig. S16. Hot stage XRD scans of the center region of aPS hot pressed at 135°C for 10min, with scans at 75°C (red), 100°C (blue), 110°C (green), 120°C (black), 170°C (pink), and 220°C (light blue). Data from 75°C - 110°C approximately concurrent, obscuring peaks.

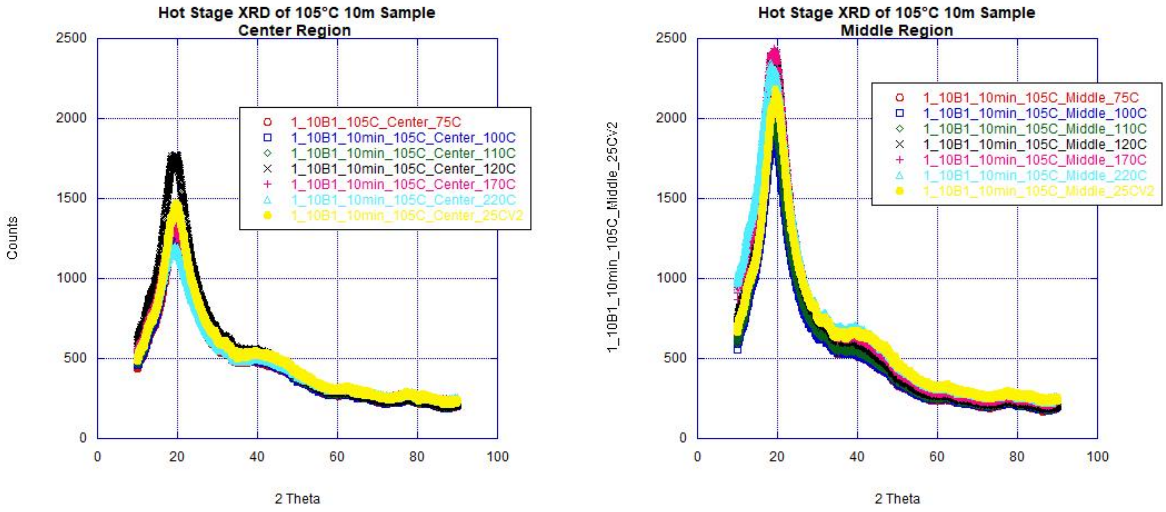

Fig. S17. Hot stage XRD scans of the center and middle regions of aPS hot pressed at 105°C for 10s, with scans at 75°C (red), 100°C (blue), 110°C (green), 120°C (black), 170°C (pink), 220°C (light blue), and then after the sample cooled to 25°C (yellow).

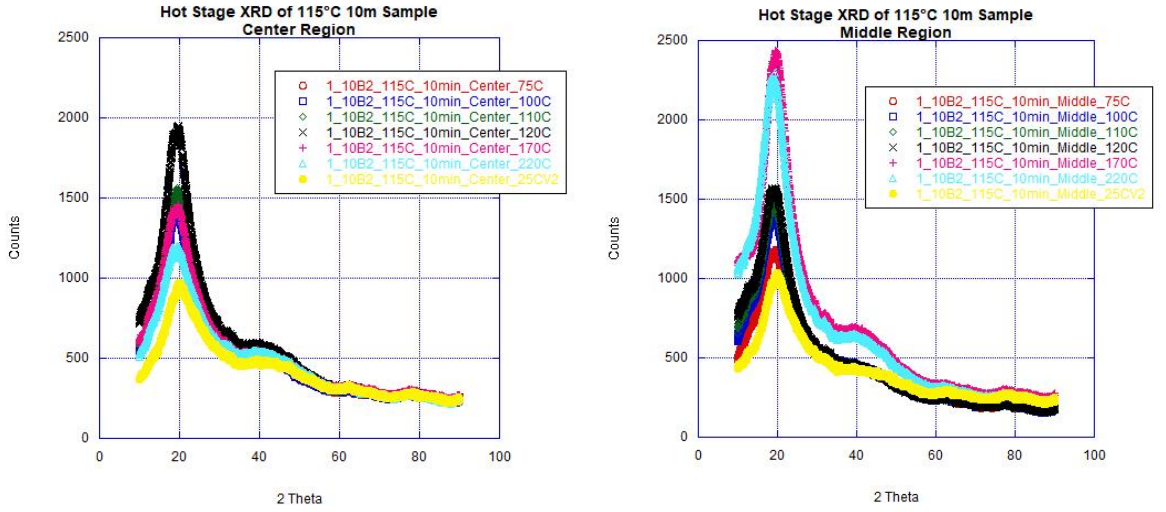

Fig. S18. Hot stage XRD scans of the center and middle regions of aPS hot pressed at 115°C for 10m, with scans at 75°C (red), 100°C (blue), 110°C (green), 120°C (black), 170°C (pink), 220°C (light blue), and then after the sample cooled to 25°C (yellow).

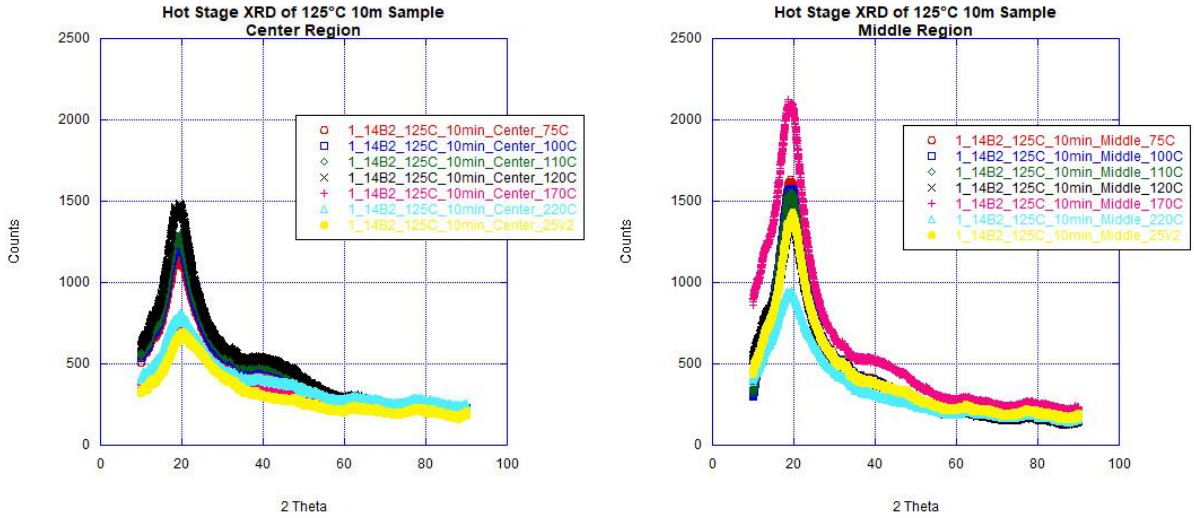

Fig. S19. Hot stage XRD scans of the center and middle regions of aPS hot pressed at 125°C for 10m, with scans at 75°C (red), 100°C (blue), 110°C (green), 120°C (black), 170°C (pink), 220°C (light blue), and then after the sample cooled to 25°C (yellow).

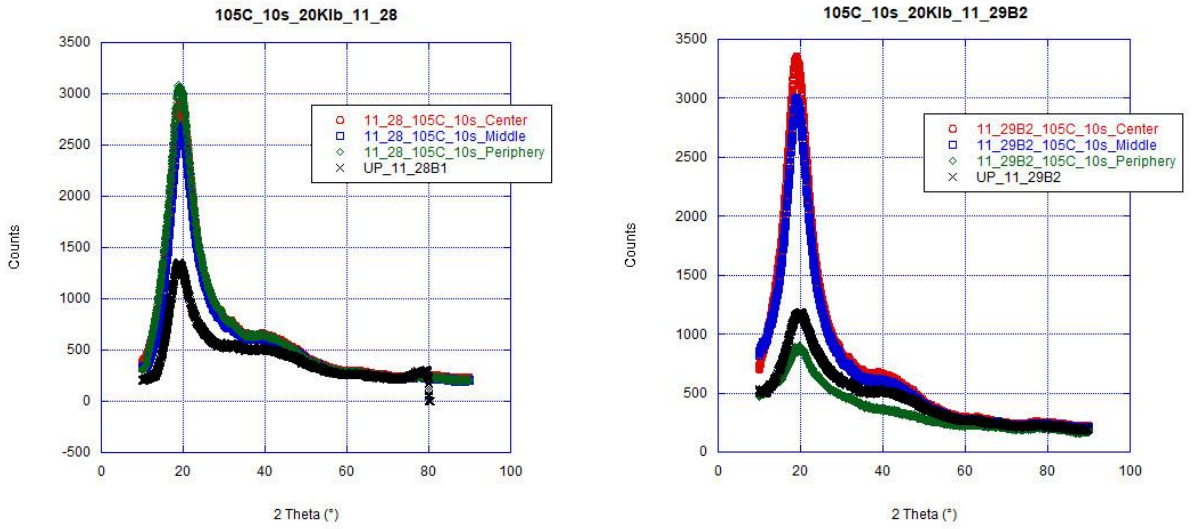

Fig. S20. XRD scans of center (red), middle (blue), and periphery (green) regions of aPS samples hot-pressed at 105°C for 10s compared to unpressed control (black).

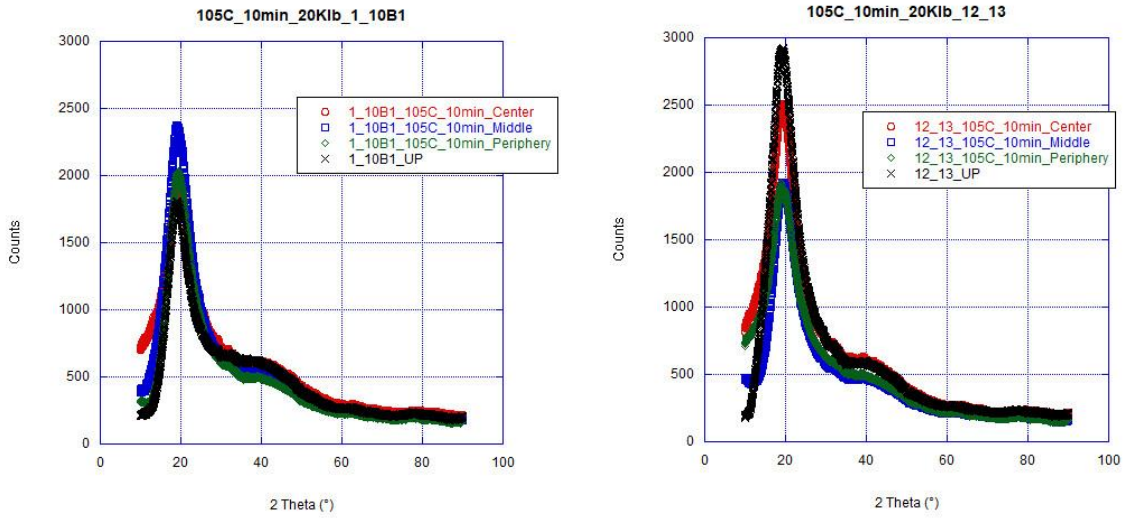

Fig. S21. XRD scans of center (red), middle (blue), and periphery (green) regions of aPS samples hot-pressed at 105°C for 10m compared to unpressed control (black).

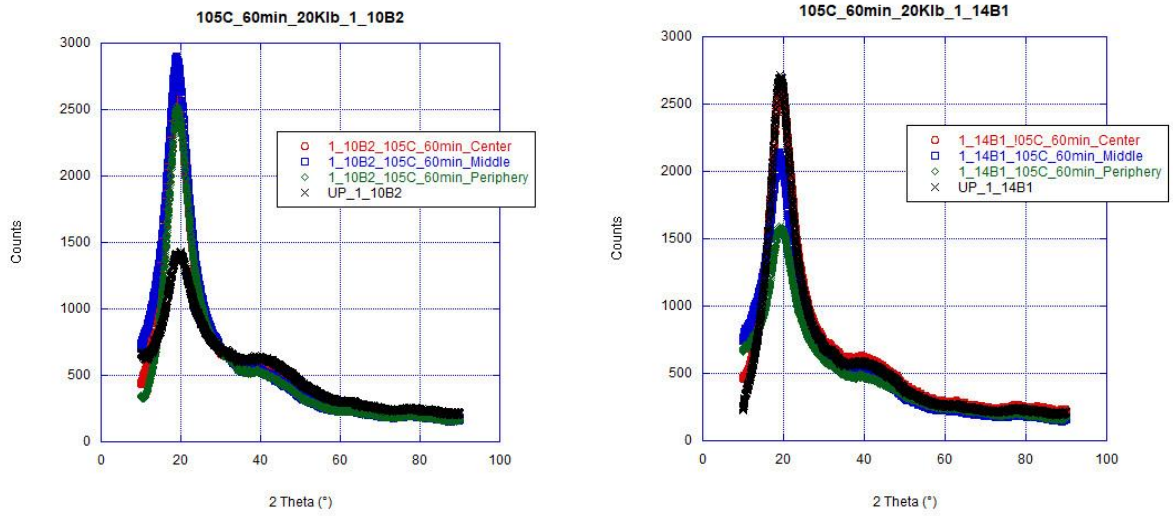

Fig. S22. XRD scans of center (red), middle (blue), and periphery (green) regions of aPS samples hot-pressed at 105°C for 60m compared to unpressed control (black).

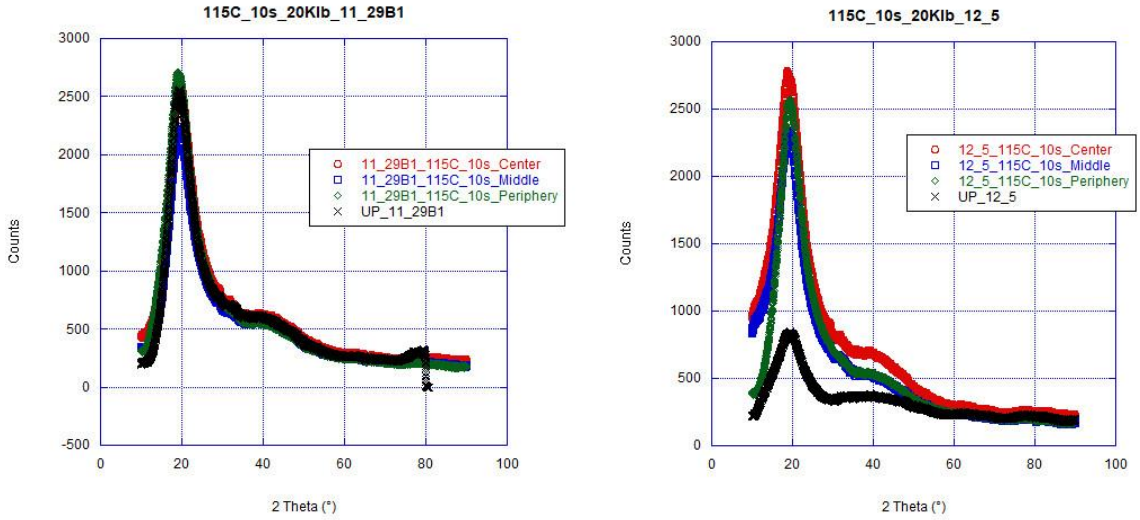

Fig. S23. XRD scans of center (red), middle (blue), and periphery (green) regions of aPS samples hot-pressed at 115°C for 10s compared to unpressed control (black).

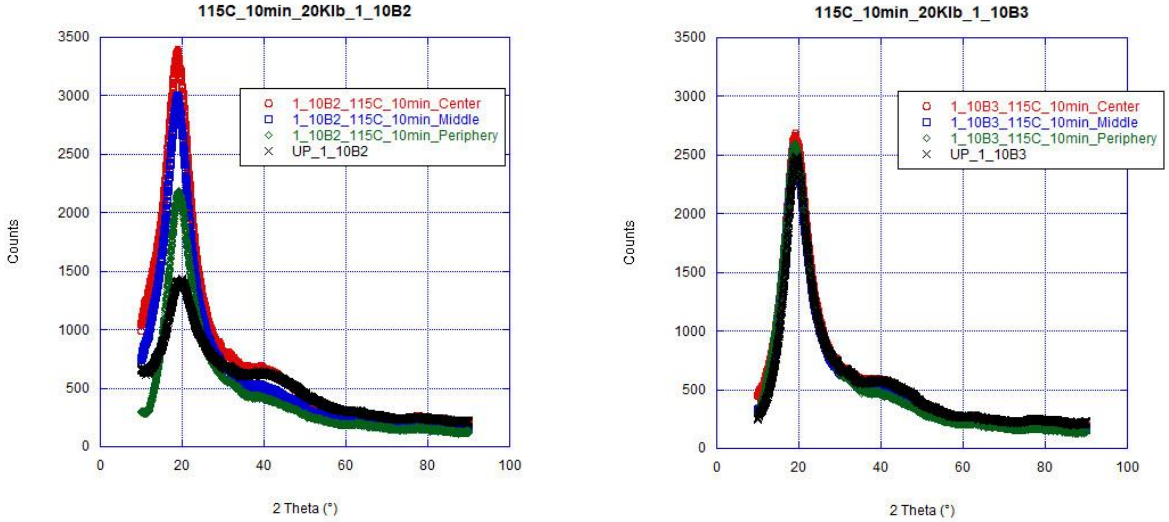

Fig. S24. XRD scans of center (red), middle (blue), and periphery (green) regions of aPS samples hot-pressed at 115°C for 10m compared to unpressed control (black).

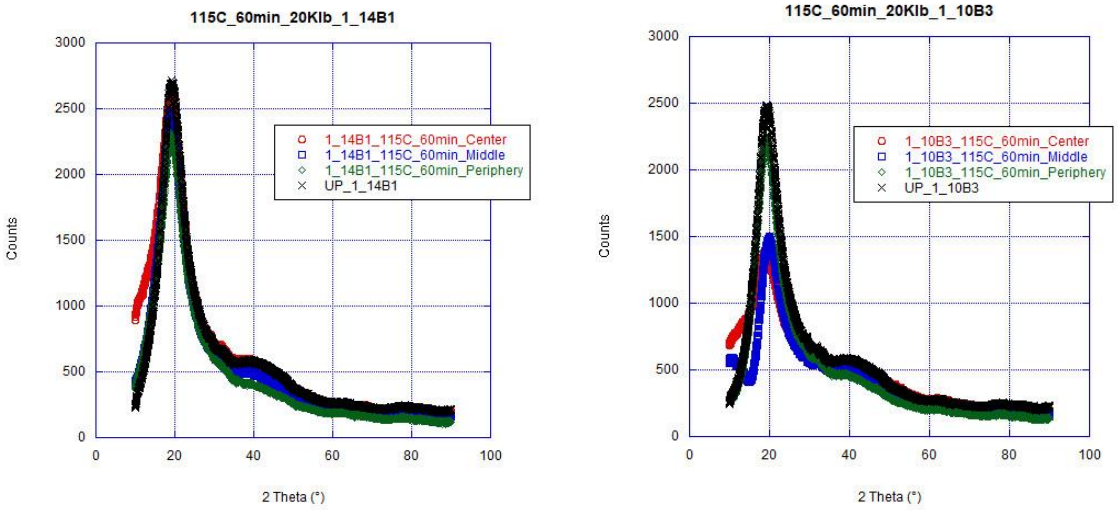

Fig. S25. XRD scans of center (red), middle (blue), and periphery (green) regions of aPS samples hot-pressed at 115°C for 60m compared to unpressed control (black).

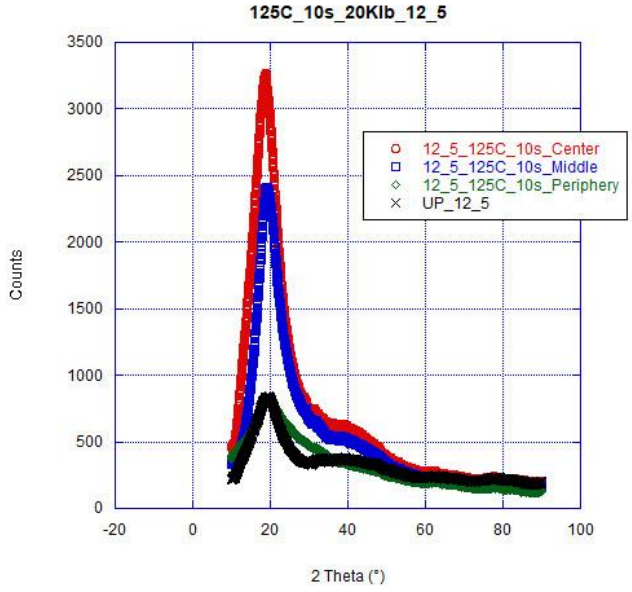

Fig. S26. XRD scan of center (red), middle (blue), and periphery (green) regions of aPS sample hot-pressed at 125°C for 10s compared to unpressed control (black).

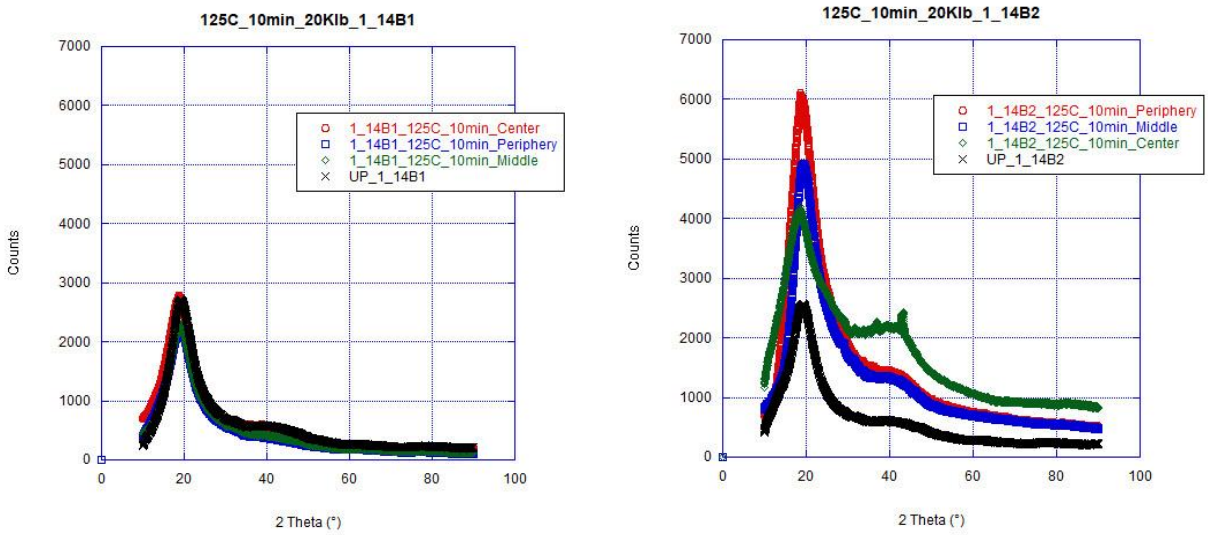

Fig. S27. XRD scans of center (red), middle (blue), and periphery (green) regions of aPS samples hot-pressed at 125°C for 10m compared to unpressed control (black).

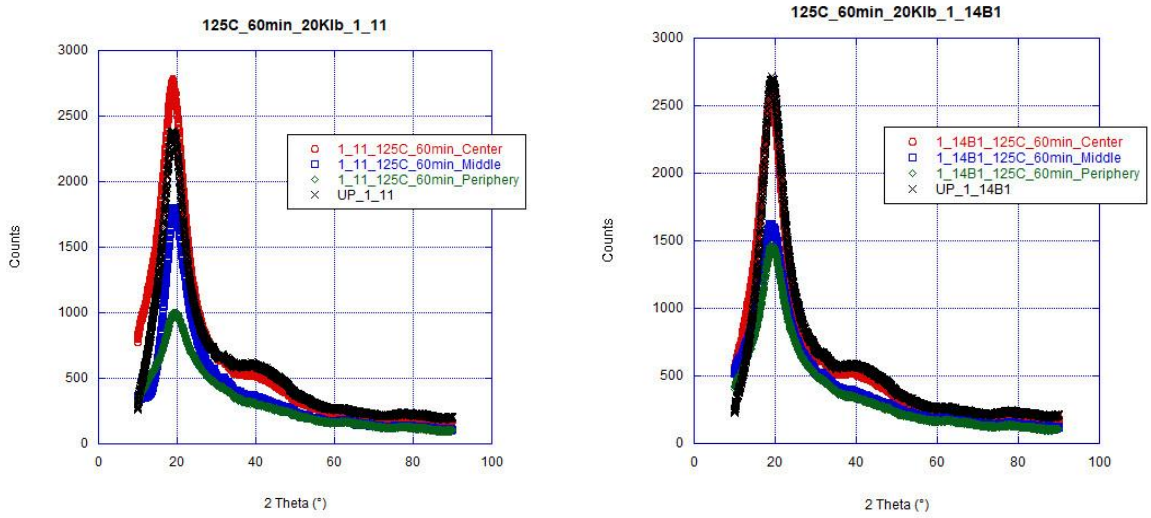

Fig. S28. XRD scans of center (red), middle (blue), and periphery (green) regions of aPS samples hot-pressed at 125°C for 60m compared to unpressed control (black).

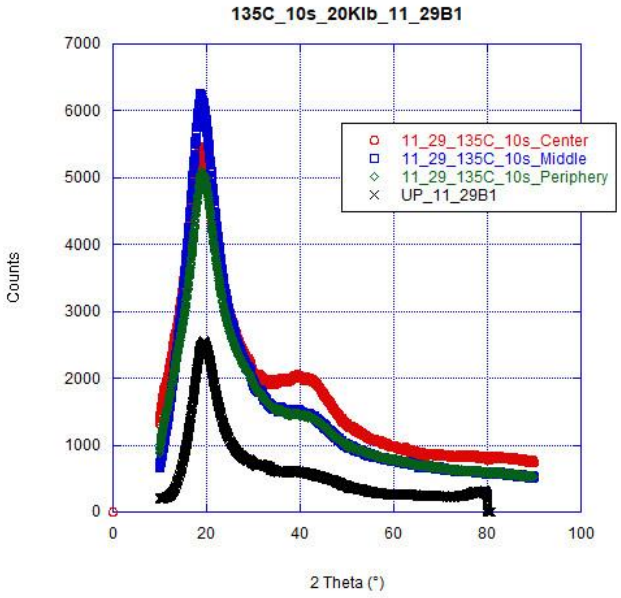

Fig. S29. XRD scan of center (red), middle (blue), and periphery (green) regions of aPS sample hot-pressed at 135°C for 10s compared to unpressed control (black).

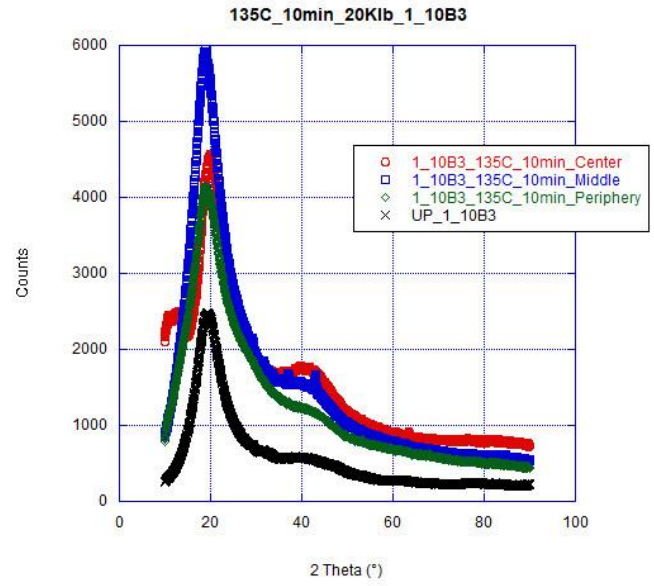

Fig. S30. XRD scan of center (red), middle (blue), and periphery (green) regions of aPS sample hot-pressed at 135°C for 10m compared to unpressed control (black).

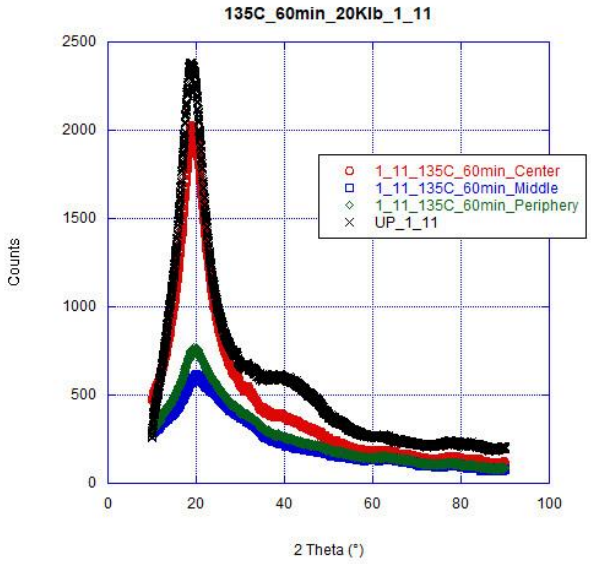

Fig. S31. XRD scan of center (red), middle (blue), and periphery (green) regions of aPS sample hot-pressed at 135°C for 60m compared to unpressed control (black).